GEOLOGY

Mid-late Pleistocene evolution of fluvial landscapes in Central Amazonia: Shaping ecosystems and areas of endemism

Cristiano P. Galeazzi[1], Renato P. Almeida[2]*, Carlos E. E. Mazoca[2], Liliane Janikian[3], André O. Sawakuchi[2], Felipe T. Figueiredo[4], Camila C. Ribas[5], Florian Wittmann[6], Fabiano N. Pupim[7]

The influence of Amazonian rivers and landscape changes on species origin and distribution remains debated. Here, we combine sedimentary, geomorphological, and chronological evidence from Central Amazonia to show that the main Amazonian rivers constructed large tracts of land that now support present-day Amazonian upland forest (terra firme). These deposits record a sequence of landscape rearrangements driven by river processes in Central Amazonia during the Pleistocene redefined the spatial boundaries of key habitats critical for many species. Our findings reveal that Amazonian rivers have acted not only as biogeographic barriers but also as powerful agents of landscape and habitat transformation, offering a unified framework for understanding how geological and biological processes together shaped the evolution of Amazonian biodiversity.

INTRODUCTION

The distribution of the extraordinary species-rich biodiversity of Amazonia has long been linked to the major river systems. Now observed biotic distributions are often bounded by the current position of river channels and their associated habitats (*1*–*4*). It is generally accepted that many patterns of current species distribution were driven by paleogeographic rearrangements involving rivers (*2*, *4*–*7*), yet the physical processes that shaped their spatial arrangement remain unclear. Current biogeographical models emphasize the role of rivers as barriers to gene flow but overlook how those same river systems have built and reshaped the landscape over time (*4*, *8*). Following the establishment of the transcontinental Amazon drainage system (*9*–*11*), which replaced extensive fluvio-lacustrine environments during the Late Miocene (*12*–*14*), the nature and timing of subsequent landscape modifications remain poorly understood.

An ongoing debate on the interaction between landscape changes and biotic distribution centers on the question of whether Amazonian rivers acted primarily just as persistent barriers to gene flow, constraining dispersal of populations, or if they were engines of speciation, through dynamic evolution and reorganization (*4*, *8*, *15*–*26*). One key area to investigate the relation of landscape changes and species distribution is Central Amazonia (Fig. 1A), where the extensive lowlands host the record of mid-late Pleistocene alluvial deposits (*27*–*29*) and well-known areas of endemism, now bounded by major rivers (*2*, *6*, *30*). Genetic evidence indicates that diversification of clades that have species on these distinct areas occurred mainly during the Pliocene-Pleistocene (*6*, *17*, *19*, *30*–*32*), providing a framework for the integration of geological and genetic studies on the distribution of Amazonian biota (*8*, *33*).

The lowlands of Central Amazonia comprise two main geomorphological elements that support distinct ecosystems (Fig. 1B): Elevated interfluves, standing several meters above river level and never flooded by rivers, support nonflooded terra firme, while river valleys, lying at flood stage elevation, host the wetlands and the seasonally flooded environments, such as várzea and igapó (*34*, *35*). Many Amazonian species are habitat specialists associated with one of these types of habitats (*36*). Species that define areas of endemism (Fig. 1C) are typically associated with terra firme habitats, such as primates (*1*, *15*, *32*, *37*) and especially birds (*6*, *7*, *19*, *30*, *31*, *38*–*40*). The boundaries of these areas of endemism are associated not only with the presence of major rivers but also with their respective wide river valleys and floodplains, covered by seasonally flooded habitats (várzea and igapó) (*4*, *37*, *41*). Thus, reconstructing how these interfluves formed and large rivers evolved during the past few hundred thousands of years is key to understanding current biogeographic patterns.

The interfluves of Central Amazonia exhibit key geomorphological and sedimentological features that record past fluvial dynamics, preserved within basin-scale sedimentary deposits accumulated between the Guianan and Brazilian shields and uplifted Subandean regions (Fig. 1A). Notably, the sedimentary deposits of these interfluves are organized into a sequence of fluvial terraces, where each lower level represents a younger depositional surface (*28*, *29*). Satellite imagery and digital elevation models (DEMs) reveal that terrace surfaces exhibit curved ridges, interpreted as scroll bars, which are depositional features produced by river channels (*42*–*44*). These structures are common in modern rivers (*45*), but their occurrence on interfluve surfaces brings new possibilities to interpret the evolution of this region. Previous interpretations have used these scroll bars to infer paleochannel positions (*28*, *44*), but there are major implications that have not been addressed so far, related to the scale of these scroll bars, which is indicative of the magnitude of the rivers that formed them (*46*–*48*), and to their elevation, which indicates that they were formed at a higher base-level position than the modern (*49*).

[1]State Key Laboratory of Oil and Gas Reservoir Geology and Exploitation, Chengdu University of Technology, Chengdu, China. [2]Instituto de Geociências, Universidade de São Paulo, Rua do Lago, 562, Cidade Universitária, São Paulo, SP 05508-900, Brazil. [3]Departamento de Ciências do Mar, Universidade Federal de São Paulo, Rua Carvalho de Mendonça, 144, Santos, SP 11070-100, Brazil. [4]Departamento de Geologia, Programa de Pós-graduação em Geociências e Análise de Bacias (PGAB), Universidade Federal de Sergipe, Avenida Marechal Rondon Jardim, s/n - Rosa Elze, São Cristóvão, SE 49100-000, Brazil. [5]Coordenação de Biodiversidade, Instituto Nacional de Pesquisas da Amazônia, Av. André Araújo, 2936, Manaus, AM 69060-000, Brazil. [6]Department of River and Wetland Ecology, Institute for Geography and Geoecology, Karlsruhe Institute for Technology–KIT, Josefstr. 1, 76437 Rastatt, Germany. [7]Departamento de Geografia, Universidade de São Paulo, Av. Prof. Lineu Prestes, 338, Cidade Universitária, São Paulo, SP 05508-000, Brazil.
*Corresponding author. Email: rpalmeid@usp.br

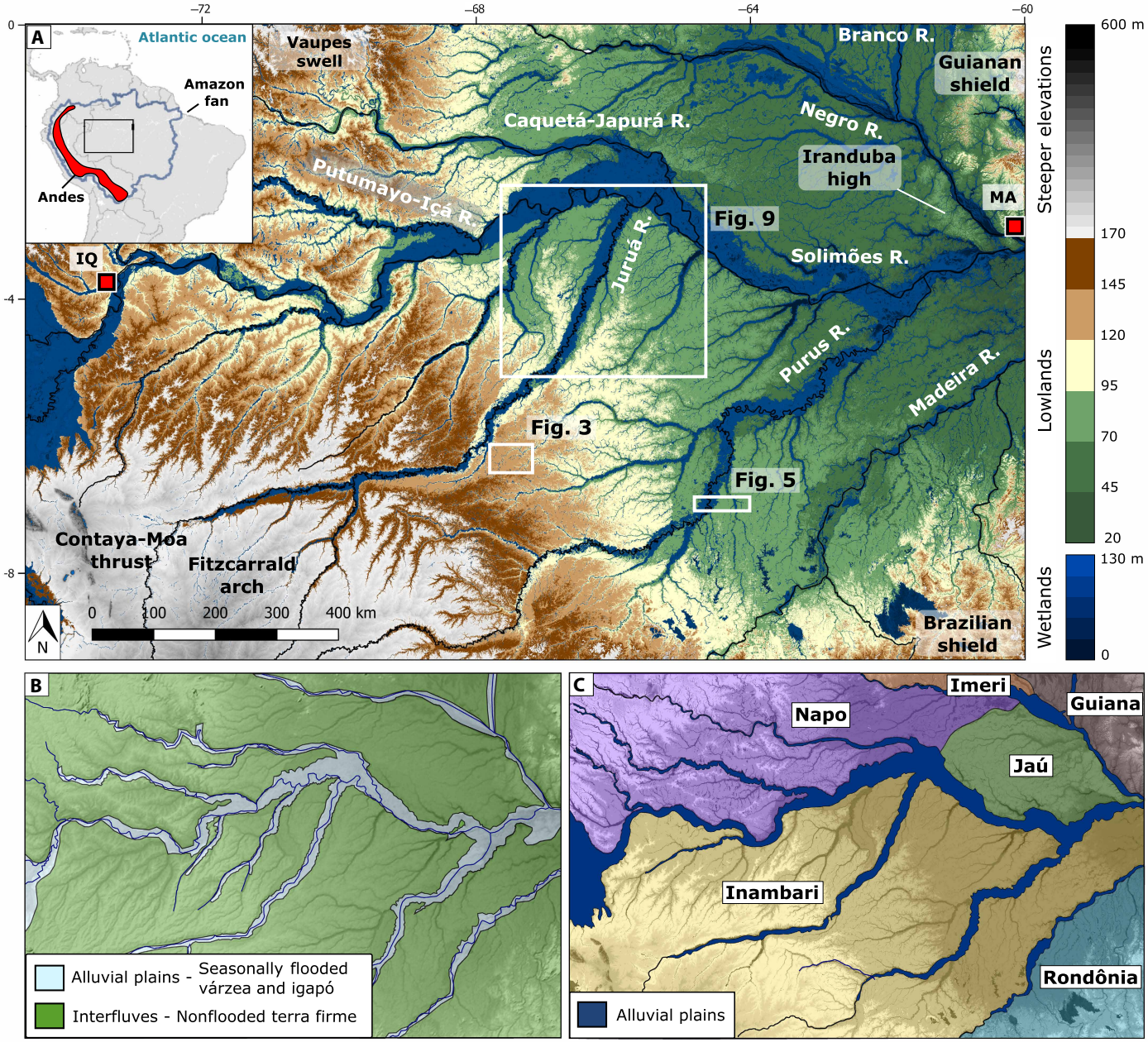

Fig. 1. Overview of Central Amazonia. (**A**) Elevation map of Central Amazonia emphasizing the variations in the alluvial terrains with key geographical features superimposed. MA, Manaus; IQ, Iquitos. (**B**) Relationship between geomorphology and type of vegetation cover illustrating the strong spatial correspondence between fluvial landforms and the distribution of flooded and nonflooded forest types. (**C**) Biogeographical areas of endemism in Central Amazonia, illustrating how major interfluves correspond to distinct biogeographic regions. Boundaries of areas of endemism follow interpretations presented in previous studies (*4*, *22*, *30*).

In this study, we reconstruct the mid-late Pleistocene evolution of the physical landscape of Central Amazonia and assess its implications for present-day biotic distribution. We examine four stages of the fluvial deposits preserved within the interfluves of Central Amazonia by a combination of remote sensing and field work and integrate these analyses with published geochronological data. The latter constrains the three youngest landscape stages to the last c. 350 thousand years (ka) (*28*, *29*, *50*–*55*), whereas the earliest stage represents an older, poorly constrained phase that is unlikely to predate ~1 million years (Ma) (*56*). We propose a new model for the paleogeographic evolution of the fluvial depositional systems in Central Amazonia, which encompasses the characterization of the paleo-rivers and the recurrent alternation between aggradational phases and events of coupled valley incision and interfluve formation through time, with implications for the spatial distribution and functioning of biotic habitats. The proposed model brings new insights to elucidate mechanisms that shaped and structured the current distribution of Amazonian biodiversity and observed areas of endemism.

RESULTS

Fluvial terrace stratigraphy and morphology

Qualitative evaluation of DEMs derived from the Shuttle Radar Topography Mission (SRTM) reveals that the interfluves of Central Amazonia comprise three main terrace stages (Fig. 2A), organized in a stepped topography where the oldest surfaces occur at the peripheral higher elevations. Each terrace consists of laterally continuous, flat surfaces gently dipping toward the valleys of the Solimões and Negro rivers. Meter-scale scarps separating adjacent terraces indicate cross-cutting relationships that allow relative chronological interpretation (Fig. 2B).

Stage I represents the oldest and highest terraces, preserved mainly along the southern, western, and northwestern basin margins. Their surfaces lie between ~150- and 100-m elevation and are deeply dissected by local drainage. Stage II forms intermediate terraces, both in elevation (100 to 40 m) and degree of dissection, typically

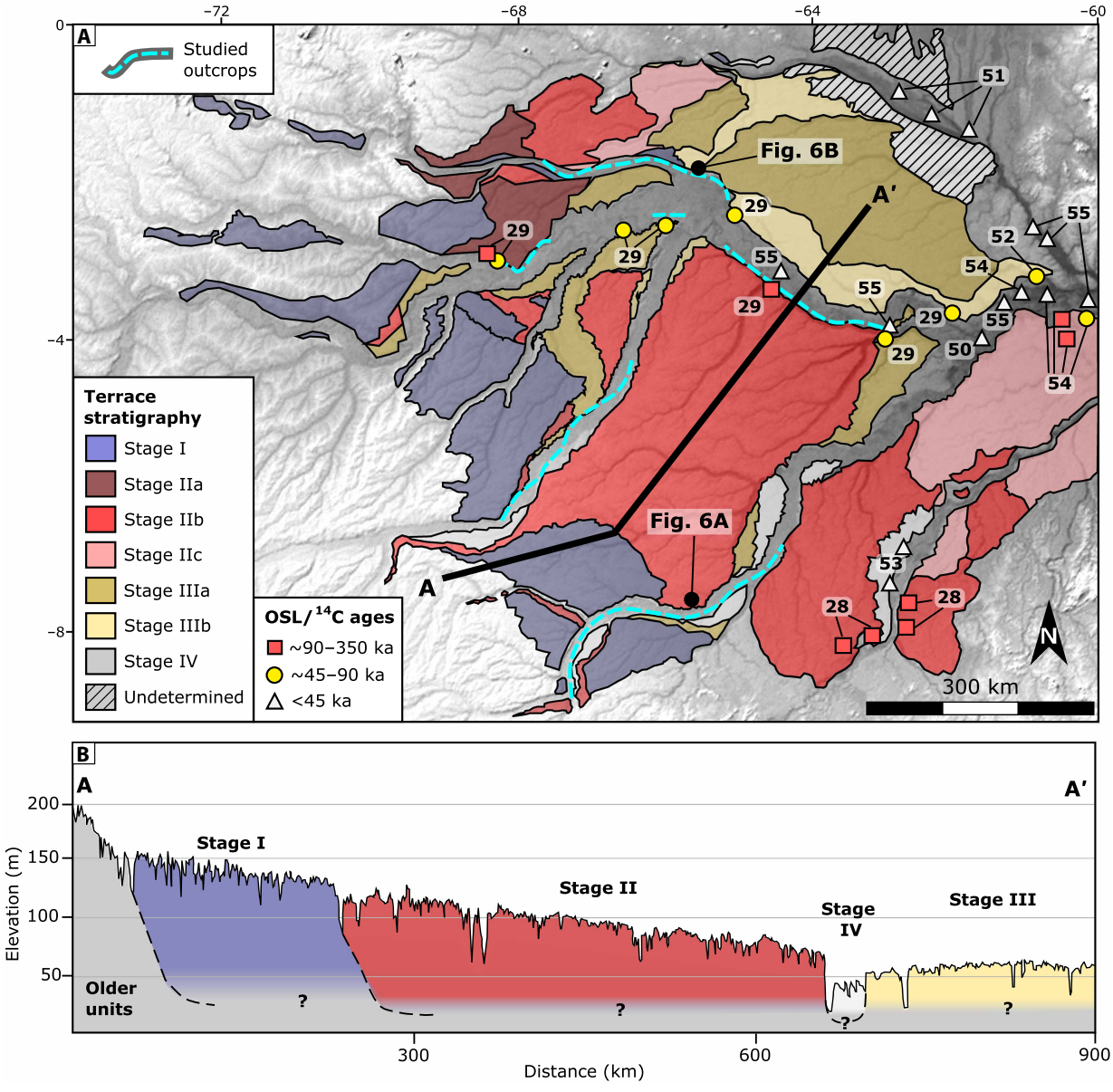

Fig. 2. Terrace stratigraphy of Central Amazonia. (**A**) The three main terrace stages (I, II, and III) and local subdivisions (designated by letters) in the same area of Fig. 1A. Light blue dashed lines indicate areas where deposits were examined in river-cut outcrops. Symbols on the map indicate chronological constraints, and the adjacent numbers correspond to their references: red squares for stage II [quartz OSL: (*28*, *29*, *54*)], yellow circles for stage III [quartz OSL: (*29*, *52*, *54*)], and gray triangles for stage IV [quartz OSL: (*29*, *52*, *54*, *55*) and ^{14}C: (*50*, *51*, *53*, *55*)]. Undetermined stages refer to low terraces that appear younger based on position but exhibit dissection typical of older surfaces. A full-resolution kmz file is available in the Supplementary Materials (data S1). (**B**) Elevation and geological profile showing stratigraphic correlations among terraces, characterized by stepped-down gentle slopes toward central regions. Question marks denote uncertainty about the strata beneath the terrace units, which may correspond to deposits that predate the studied terrace systems or remnants of older terrace stages. Note that elevations include forest canopy height, as the SRTM-derived DEM does not represent bare-earth topography.

occurring between the basin margins and the modern valley floors. Stage III corresponds to the youngest terrace level, less dissected and located near the modern Solimões River, with surface elevations of 60 to 30 m. Modern floodplains and smaller in-valley terraces represent stage IV. Each stage includes local subunits labeled with letters, without implying regional correlation, given uncertainties in absolute depositional ages. In the lowermost areas, some terraces remain undetermined because pronounced desiccation gives them the appearance of older landforms, making confident assignment to a specific stage uncertain (fig. S1).

Published geochronological data provide age constraints for the above-mentioned stages. Considering analytical uncertainties, the mapping scale, and the limited number of dated samples available for this region, the following ages should be regarded as approximate. Although stage I lacks direct dating, its stratigraphic position above uplifted Late Miocene deposits of the Fitzcarrald Arch (Fig. 1A), which was estimated to have been uplifted during the Pliocene (*57*), and its well-preserved fluvial morphology suggests a Pleistocene depositional age (*56*). Stage II terraces yield quartz optically stimulated luminescence (OSL) ages predominantly between ~90 and >300 ka (*28*, *29*, *54*). Stage III deposits are dated (quartz OSL) predominantly to ~50 to 90 ka (*29*, *42*, *54*), whereas stage IV, corresponding to modern valleys and floodplains, records deposits with quartz OSL and radiocarbon (^{14}C) ages from the Holocene to 45 ka (*29*, *50*–*55*).

Across the region, terrace successions display a systematic pattern produced by successive phases of fluvial incision, during which rivers cut into older depositional surfaces to generate progressively younger terrace levels. This incision produced narrow proximal valleys that gradually widen downstream over hundreds of kilometers into low-gradient, elongated landforms. In several areas, these paleoalluvial plains preserve fan-shaped morphologies with radii extending over hundreds of kilometers (Fig. 2).

Planform analysis of the terraces reveals clear evidence of paleoalluvial systems. Each terrace level exhibits diagnostic fluvial morphologies, including point bars, scroll bars, and abandoned channels, with individual depositional elements reaching kilometer-scale dimensions (Fig. 3). Multiple sets of paleochannels at similar elevations on the same terrace indicate episodes of regional avulsion [sensu (*58*)]. In fan-shaped terraces, paleochannels display radial arrangements originating from nodal points at higher topographic positions, consistent with large-scale distributive fluvial systems (Fig. 3).

Paleohydrology of the terrace systems of Central Amazonia

The term "terrace system," as used here, refers to a sequence of terraces derived from the same fluvial system, in which younger levels are deposited topographically below older ones in a stepwise arrangement, and whose sedimentary provenance is presumably interpreted to be the same. Terraces were grouped in eight terrace systems, according to the location and stratigraphic relationships of incisions, scale of depositional elements, and observed paleochannel directions, from where paleoflow can be inferred. Names were assigned according to the kilometer-scale depositional features, which indicate deposition from large rivers, the spatial coincidence between the locations of the incisions, and the present courses of major Amazonian rivers, namely, Solimões, Japurá, Madeira, Juruá, Purus, Içá, Jiparaná, and Aripuanã (Fig. 4). Paleoflow directions were reconstructed from the orientation of paleochannels observed in remote sensing imagery (Fig. 3) and field measurements of cross-strata. The Solimões, Japurá, and Içá systems show eastward paleoflow; Juruá and Purus trend northeastward; Madeira is northward; and Jiparaná and Aripuanã are northwestward (Fig. 4). The terrace systems of the Solimões, Japurá, Madeira, and Juruá account for most of the exposed surfaces and preserve abundant scroll bars suitable for quantitative morphometric analysis.

To assess the discharge scale of the paleo-rivers, the radii of curvature of scroll bars were measured and compared with those from modern rivers and small tributaries incised into the same interfluves (Fig. 5). Scroll bars within the active floodplains of large Amazonian rivers (Solimões, Japurá, Madeira, and Juruá) exhibit large-scale curvature radii, with 75% exceeding 2000 m, whereas small tributaries display radii consistently smaller. On the other hand, scroll bars preserved on the terrace surfaces show large-scale curvature radii with more than 75% exceeding 2000 m, matching those of modern large rivers rather than local tributaries. The Paleo-Solimões terrace system exhibits the largest preserved scroll bars, followed by the Paleo-Madeira, Paleo-Juruá, and Paleo-Japurá systems. Except for the Paleo-Juruá, the size of scroll bars in the terrace systems closely resembles their modern counterparts.

Statistical comparisons of scroll bar radii of curvature further support these interpretations (table S1). In all terraces, paleo-major rivers and their modern counterparts show small differences in mean curvature (fold change of ~1 in Japurá, Solimões, and Madeira rivers and ≤2 in Juruá River), whereas contrasts between paleo-major rivers and modern local tributaries exhibit order-of-magnitude differences (fold change of 5 to 13). Normal tests on mean curvature radii yield $P < 0.001$ for all comparisons, indicating significant differences in central tendency. However, Kolmogorov-Smirnov (KS) tests reveal that paleo-river distributions closely resemble the modern mainstem rivers ($D = 0.10$ to 0.51, $P = 10^{-5}$ to 10^{-87}) but are highly distinct from the local tributaries ($D = 0.97$ to 1.0, $P < 10^{-160}$). These results demonstrate that the entire distribution of curvature radii in the terrace systems aligns with the scale of modern large rivers rather than small rivers. Thus, the preserved scroll bar systems record the planform geometry of high-discharge Paleo-Solimões, Paleo-Madeira, Paleo-Juruá, and paleo-Japurá rivers (fig. S2).

Sedimentology of terraces

Exposures on modern river cuts reveal sections of these terraces. The interpretation of the terrace vertical exposures supports the kilometer-scale nature of the depositional elements described above. Two main facies associations are recognized from the observed facies (figs. S3 and S4) in these outcrops: large-scale sandy bars deposits (FA1) and floodplain deposits (FA2) (table S2). These exposures may be tens of meters high and hundreds of meters long (Fig. 6).

FA1: Large-scale sandy bar facies association

The deposits forming FA1 are dominated by fine to coarse sands with granules, characterized by the predominance of decimeter-scale cross-strata sets and fining up sequences that may reach 20 m in thickness. At their bases, granule and pebble-sized mud clasts are frequent within meter-scale cosets of inclined decimeter-scale cross-strata sets [compound cross strata-sets; (*59*, *60*)], whereas the upper portions gradually transition into finer-grained beds. Submetric silt and clay lenses, commonly less than 25-cm thick and laterally continuous for less than 100 m, occur mostly in the upper part of the sections (Fig. 6A). These bodies may display internal large-scale low-angle inclined surfaces, forming meter-scale inclined beddings, with internal decimeter-scale cross-stratified sets. These surfaces may display decimeter-scale lenses of mud (fig. S5A). Measurements of cross-strata orientation from

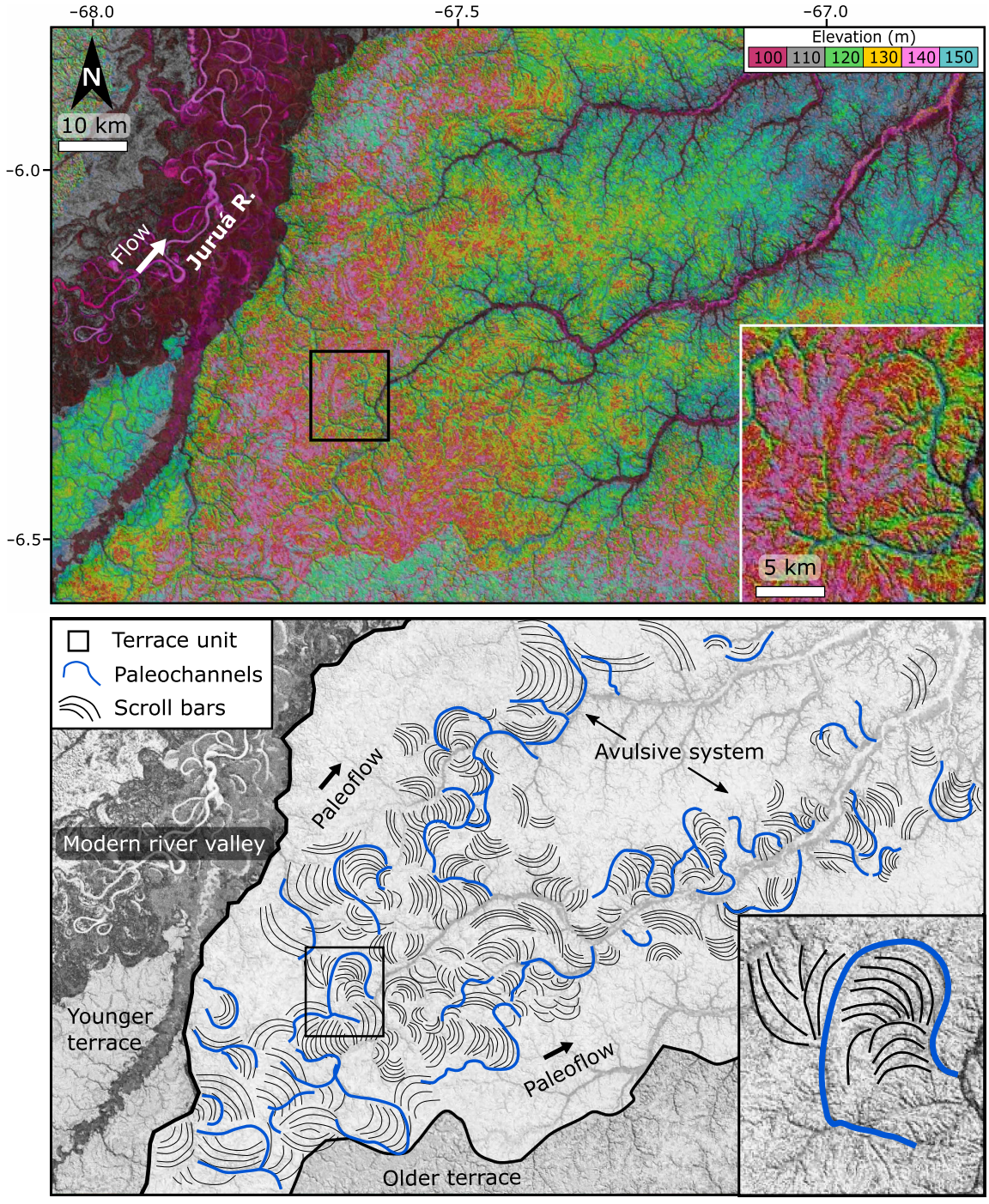

Fig. 3. Evidence of avulsion-dominated fluvial deposition in paleo-alluvial plains. DEM of the stage II terrace of the Paleo-Juruá alluvial plain and the respective interpreted image. The interpreted image depicts kilometer-scale scroll bars preserved on the surface of the terrace characterizing a fan-shaped terrace with a radial avulsive system stemming from a nodal point, whose location is roughly coincident with the inset box. Inset boxes illustrate in detail a meander of the paleo-channel, with its respective scroll bars. See location in Fig. 1.

this facies association were taken at several locations in each terrace system, yielding a spatial distribution of river paleoflow directions. The Solimões and Japurá terrace systems display a relatively low angular dispersion of individual paleocurrent measurements around the mean paleoflow direction, whereas the Madeira and Juruá terrace systems exhibit substantially higher paleoflow dispersion (Fig. 4).

The 5- to 20-m-thick, fining-up sequences imply several meters-deep channels at the time of deposition. Coarse-grained inclined cosets are interpreted as the product of large compound dunes with superimposed dunes on the leeside that occur at the base of large rivers (Fig. 6A) (*59*–*61*). Large-scale inclined beddings draped by mud lenses with internal cross-stratification are interpreted as surfaces of

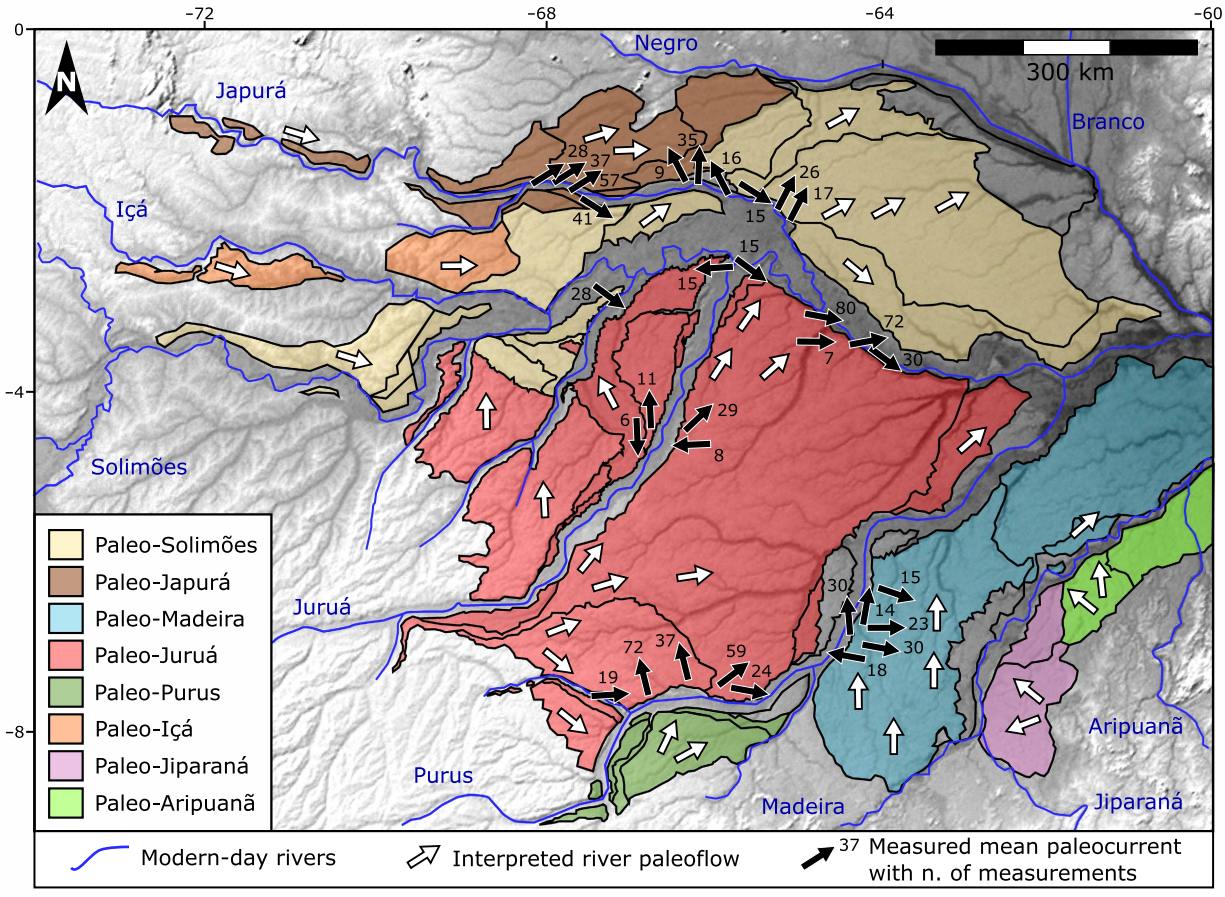

Fig. 4. Map of deposits attributed to major paleo-Amazonian rivers. Interpreted river paleoflow map for terrace systems of stages I, II, and III. White arrows point to the reconstructed flow directions based on preserved scroll bars observed from the surface of the terraces through the analysis of the SRTM-based DEM. Black arrows represent the mean paleocurrent direction measured in several locations of the terrace systems from outcrops during field work. Dispersion of paleocurrent directions reflects spatial variability in flow orientation across terrace systems.

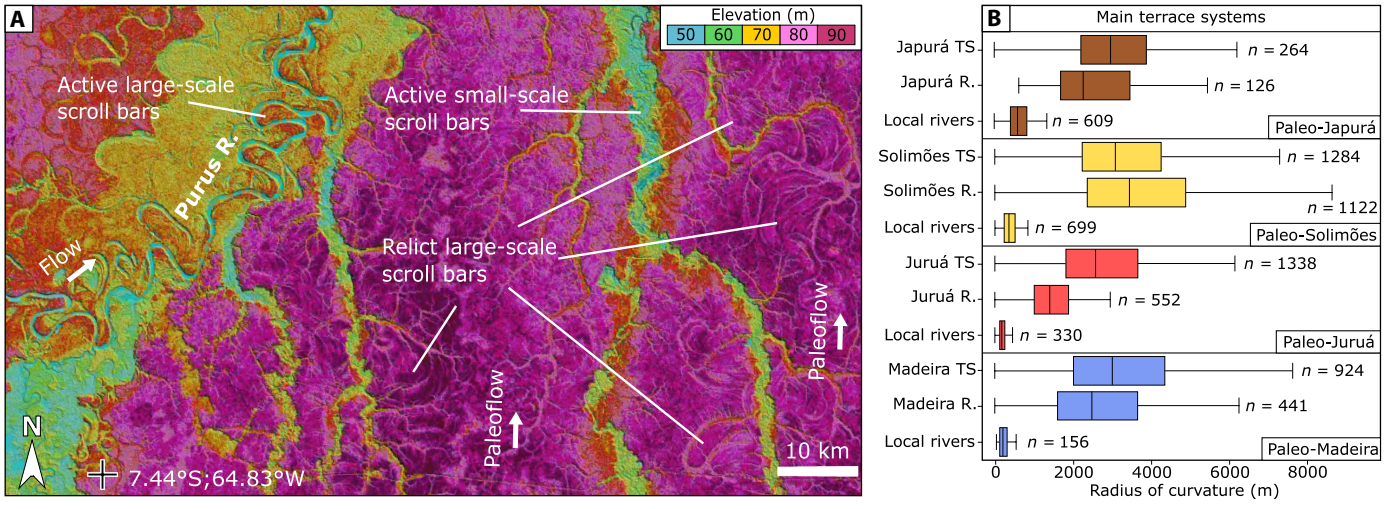

Fig. 5. Comparison of mid-late Pleistocene and modern scroll bars. (**A**) DEM shows scroll bars on the surface of the Purus-Madeira interfluve (pink), which are much larger than those found in the modern small tributaries in the same area (green to blue), and of similar scale to the ones found in the Purus modern in-valley alluvial plain (pale orange). (**B**) Boxplots comparing radii of curvature of scroll bars preserved on the major terrace systems (TS) of Central Amazonia, on modern alluvial plains of their respective major Amazonian rivers, and on the alluvial plains of small local tributaries (labeled as "local rivers"). The scale of scroll bars preserved on the terrace surfaces aligns with those of major rivers (Solimões, Madeira, Japurá, and Juruá rivers) rather than to the small, low-discharge tributaries that presently occupy the interfluves surface. See location in Fig. 1.

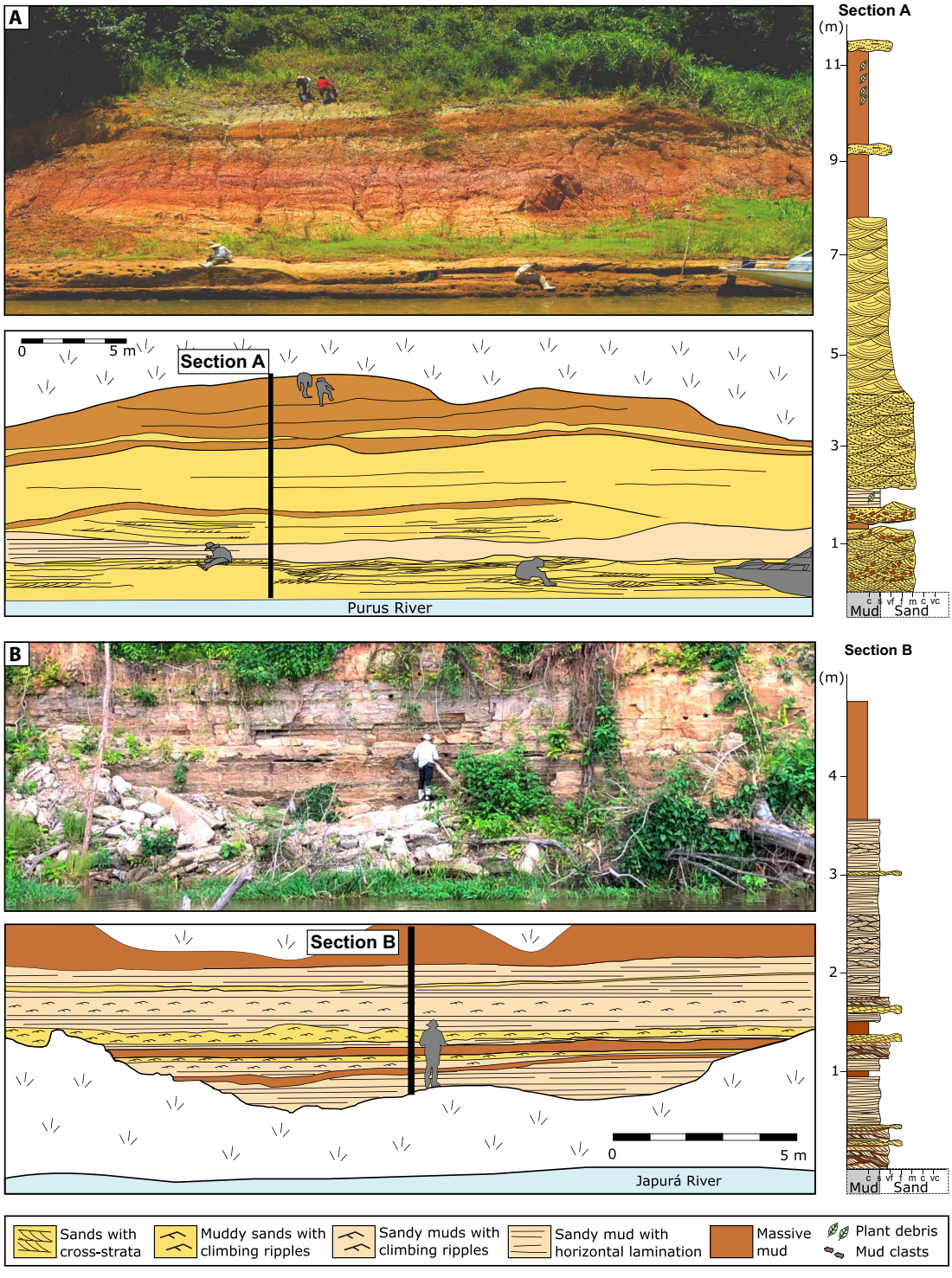

Fig. 6. Representative outcrops of mid-late Pleistocene terraces of sandy bars and floodplain deposits. (**A**) Fluvial sandy bars deposits (FA1) in the Purus River: meter-scale thick fining-upward sequence, with large-scale scours and mud clasts at the base and dominated by decimeter-scale cross-bedded sands, overlain by a succession of mud layers. (**B**) Floodplain deposits (FA2) in the Japurá River: interbedded mud and fine sand with the occurrence of climbing ripples in fine sand and sandy mud. Location of outcrops is indicated in Fig. 2. c, clay; s, silt; vf, very fine; f, fine; m, medium; c, coarse; vc, very coarse.

lateral or oblique accretion of bars at the margins of the channel, where mud lenses may be related to deposition during waning stages of the river (fig. S5A). The sedimentological interpretation of the dominant sandy bars facies association agrees with the plan view pattern of large river deposits described above, revealing the deposits of large-scale sandy bars of 10 to 20 m, formed by deep, large rivers, similar to those in the active large rivers in the same region (*59*–*63*). The measured paleocurrent directions are consistent with the general flow of each terrace system, interpreted from the paleochannels in a plan view of the terrace systems. The mean river paleoflow direction in the Solimões and Japurá terrace systems has a lower dispersion around the mean river paleoflow direction than the Madeira and Juruá terrace systems (Fig. 4). This contrast reflects differences in the spatial variability of paleoflow directions across the terraces and may be attributed to differences in paleo-channel sinuosity, with lower-sinuosity systems producing more uniform paleoflow directions and higher-sinuosity systems generating greater directional variability (*45*).

FA2: Floodplain deposits facies association

The deposits forming this facies association are characterized by fine-grained sediments displaying laminated sandy mud, which may have abundant plant remains, or laminated heterolithic bodies of fine sand, silt, and clay, but meter-scale beds of centimeter-scale sets of cross-laminated silt also occur, as well as decimeter-thick fine to medium sand lenses rich in mud clasts (Fig. 6B). In some sections, several-meters-thick successions of muddy silt display inclined, internally laminated sets or climbing ripples at the base that progressively coarsen upward into decimeter-scale intercalations of cross-bedded fine to medium sand and mud (fig. S5B).

These horizontally laminated fine-grained deposits mostly depict sedimentation in an environment of stagnant water or stagnant water with intermittent currents that bring slightly coarser-grained sediments. Fine-grained deposits with cross-lamination represent the deposits of climbing ripples formed during flow deceleration coupled with aggradation. Whereas the sand bodies with mud clasts are interpreted as floodplain channels (Fig. 6B). The fine-grained successions found with inclined sets of muddy silt in outcrops of the modern Solimões River record wide submerged floodplain environments, similar to the great floodplain lakes flanking the modern-day Amazon River downstream of the Negro River junction, and the coarsening upward trend is interpreted as the successive stages of progressive infill of such lakes (*64*). The thickness of these sequences further provides important constraints on the scale of the fluvial systems to which they are related (fig. S5B).

DISCUSSION

Dynamic alluvial systems of Central Amazonia during the mid-late Pleistocene

Understanding the configuration and evolution of Pleistocene alluvial systems is essential for reconstructing how the modern Amazonian landscape and its zonation in seasonally flooded (várzea and igapó) and upland (terra firme) ecosystems came to be. These systems record the processes by which large rivers repeatedly reshaped the lowlands, influencing the distribution of seasonally flooded and nonflooded environments that underpin the region's present-day biogeography. Although a transcontinental drainage was already established by the Late Miocene (*9*, *10*, *12*), the landscape of the topographically depressed region of Central Amazonia remained far from static during the Pleistocene (*29*, *65*). Instead, sedimentary, geomorphological, and stratigraphic evidence reveal that this region underwent major reorganization during the mid-late Pleistocene, as large river systems avulsed across broad unconfined plains and progressively infilled the basin with extensive alluvial deposits (Fig. 7).

The stratigraphic record corresponding to the time interval between the Late Miocene establishment of the transcontinental Amazon River, at c. 9 to 12 Ma (*8*, *9*, *11*), and its modern drainage configuration is scarce and only partially preserved in subsurface sedimentary successions [e.g., (*66*, *67*)]. It is largely inaccessible in outcrops across Central Amazonia, where exposed successions mostly correspond to the overlying, younger Pleistocene alluvial deposits studied herein. Throughout this interval, subsurface studies from cores interpret the presence of extensive wetlands and fluvial systems (*68*), and provenance analysis in one core in the western portion of Central Amazonia shows that detrital zircon populations are comparable to the modern Amazon River (*69*), indicating that the mid-late Pleistocene alluvial systems analyzed here can therefore represent the latest phase of a long-lived, dynamically evolving fluvial landscape.

The preserved mid-to-late Pleistocene deposits (Fig. 2) record at least eight extensive alluvial systems, likely corresponding to the ancestors of the modern large Amazonian rivers (Fig. 4). Kilometer-scale depositional elements (Fig. 3), terrace scroll bar radii of curvature (Fig. 5), and vertical facies successions (Fig. 6) indicate that these paleo-rivers were comparable in scale to the modern large Amazonian rivers but operated at higher base levels. The Paleo-Solimões and Paleo-Madeira plains display roughly parallel paleochannels and alluvial ridges, whereas the Paleo-Japurá, Paleo-Juruá, Paleo-Içá, Paleo-Purus, Paleo-Jiparaná, and Paleo-Aripuanã systems exhibit fan-shaped morphologies with radial paleochannels. The Paleo-Solimões and Paleo-Madeira likely functioned as the principal trunk rivers, while systems such as the Paleo-Japurá, Paleo-Juruá, and Paleo-Purus formed large megafans (*70*) draining into them. These interpretations derive from preserved paleoflow directions (Fig. 4) and scroll bar radii of curvature (Fig. 5), the latter indicating that the Paleo-Solimões and Paleo-Madeira had the largest paleo-discharges. Paleogeographically, the Paleo-Solimões, Paleo-Japurá, Paleo-Içá, and Paleo-Madeira systems likely drained directly from the Andes, whereas the Paleo-Purus and Paleo-Juruá originated east of the Subandean thrust front, on the Fitzcarrald Arch (Fig. 1A), where their terraces are incised (Fig. 2A), similar to their modern counterparts, indicating broad continuity in basin-scale organization. The Paleo-Negro is also interpreted to have been a trunk river. Although no alluvial deposits attributable to the Paleo-Negro have been identified, its presence is inferred by the northeastward paleoflow orientations of the Paleo-Solimões and Paleo-Japurá, which must have ultimately converged along the course of the modern Negro River. The lack of preserved deposits likely reflects the draining of low–sediment yield crystalline terrains of the Guiana Shield (*71*), which supplied predominantly suspended load that was transported through the system rather than stored as aggradational plains.

Modern analogs for these paleo-systems include the Bermejo and Pilcomayo Rivers, which form narrow, confined megafans, and the Pastaza, Kosi, and Paraná megafans, which display broad radial distributive geometries (Fig. 8) (*70*, *72*). Avulsive channel migration likely occurred on centennial- to millennial-scale timescales (*50*, *58*, *73*, *74*). The resulting depositional architecture, from stage I (>350 ka) to stage III (until 45 ka), reflects a landscape dominated by aggradational, avulsion-controlled river systems rather than the erosive river valleys separated by upland interfluves seen today.

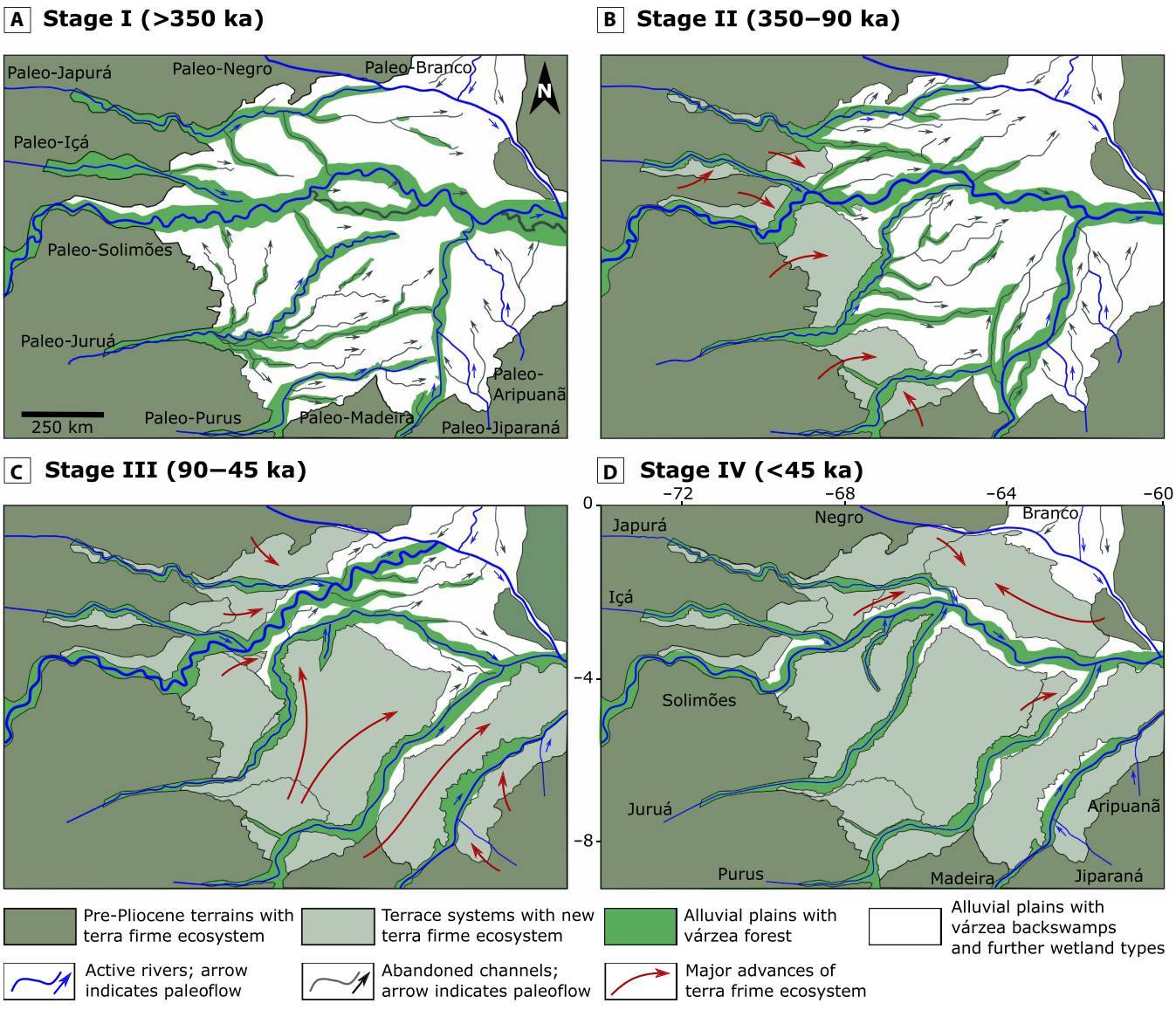

Fig. 7. Evolution of mid-late Pleistocene physiographic and biotic landscapes in Amazonia. (**A**) Stage I depicts widespread aquatic and seasonally flooded environments, with the lowlands displaying the extensive alluvial plains of all the paleo-river systems. Alluvial plains mainly comprise vegetation adapted to seasonal flooding, such as várzea forests, backswamps, and nutrient-poor swampy regions. (**B**) Stage II records the first major base-level drop, characterized by terrace formation from the eastern and southern margins, coupled with the expansion of terra firme ecosystem. Sedimentary wedges formed by the paleo-megafans occupy more central regions. (**C**) Stage III depicts a second major lowering of the base-level and is characterized by an extensive area of terrace formation and further expansion of terra firme forest, especially south of the modern-day Solimões River. During this stage, the Paleo-Solimões River flows toward the Paleo-Negro River, meeting it upstream of the modern-day point of confluence. During stage IIIb, terra firme occupied the terrace in the central region, spreading from the Iranduba High (Fig. 1A). (**D**) Stage IV illustrates the final configuration before the establishment of the modern drainage network, after the capture of the Solimões River by a knickpoint from the east. Note that courses of paleo-rivers and extension of várzea forest at their margins are schematic.

The down-stepping geometry of the Central Amazonia terraces (Fig. 2) records successive base-level drops, each marking a shift from widespread sedimentation to valley incision and floodplain abandonment: The higher interfluves relative to modern valleys indicate deposition under higher base levels, and their cross-cutting relationships attest that each avulsive phase ended with base-level fall and valley incision, which lead to subsequent erosive widening. Terraces at various elevations thus represent diachronic alluvial systems formed in response to cycles of rising and falling of the base level (Fig. 2).

Each base-level fall followed a similar pattern (Fig. 9): Starting from wide avulsive plains and megafans (Fig. 9A), base-level lowering caused rapid valley incision of major tributaries. Former floodplains became terraces, incision propagated upstream, and valley knickpoints retreated through tributaries (Fig. 9B). Once the base level stabilized, rivers reestablished distributive patterns in unconfined areas, depositing a new sedimentary wedge that prograded from the basin margins toward its central depression, forming new alluvial plains. Repeated base-level falls produced a stepped topography

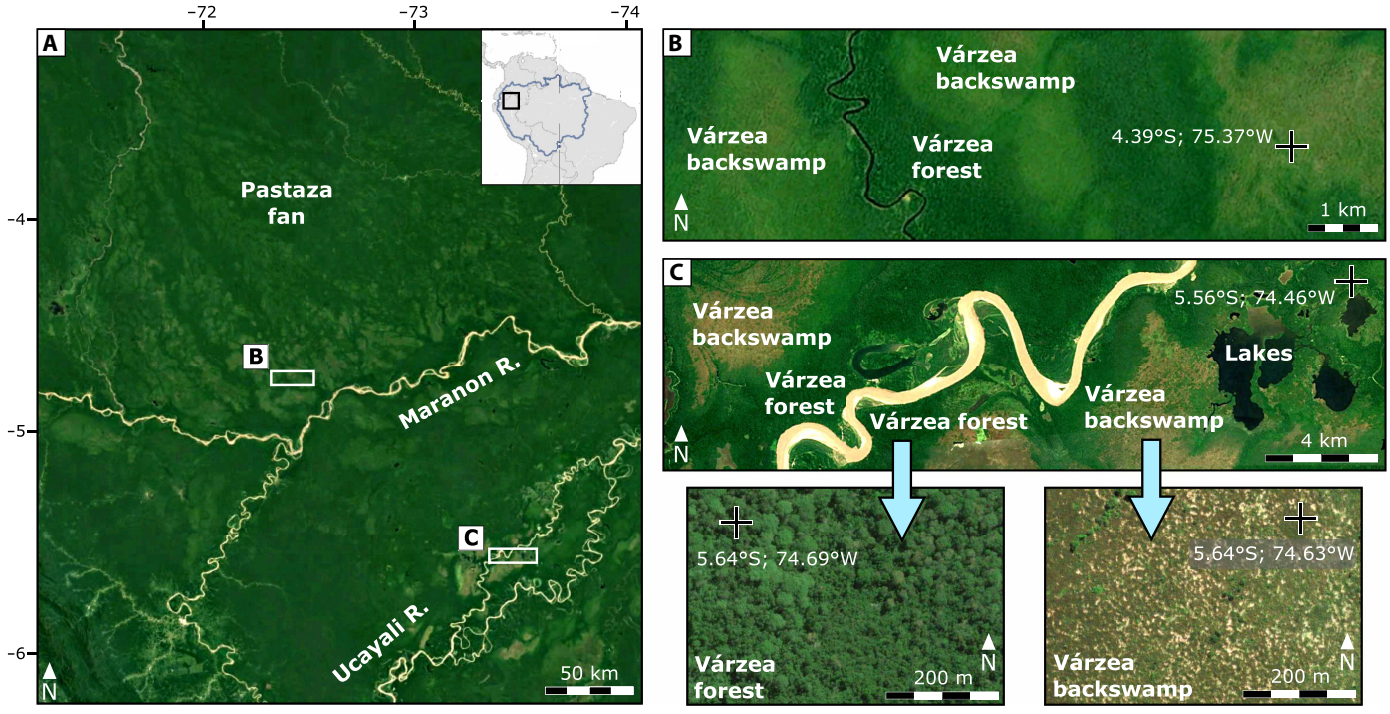

Fig. 8. Modern avulsion-dominated alluvial plain in Amazonia (Ucayali River and Pastaza Fan, Peru). (**A**) Overview of the area encompassing the Pastaza Fan and the Ucayali River. (**B**) Detailed view of the Pastaza Fan. (**C**) Detailed view of the Ucayali River. In both examples, the várzea forest is restricted to areas near the main channels, whereas backswamps dominate more distal areas of the floodplains. Images of (A) to (C) are from Google Earth; zoom-ins of (C) are from Bing Maps.

of nested terraces (Fig. 9C). Knickpoint retreat may also have triggered river capture, as observed in the modern Juruá course (Fig. 9, B and C) (*44*). This process likely repeated during the stage IV course change of the Solimões River (Fig. 7D) and the capture of the Juruá headwaters by the Purus River, which now has a higher discharge than the Juruá River, explaining the difference of scroll bar size observed in the Paleo-Juruá River compared to the modern-day Juruá River (Fig. 5).

From stage I to stage III, the Amazonian lowlands thus functioned as vast, distributive fluvial systems characterized by frequent avulsion and lateral channel mobility. An overall net base-level lowering influenced the basin infill of the basin though sedimentary wedges that prograded from the margins toward its central depression. This evolving alluvial landscape provides the tools for understanding the subsequent paleoenvironmental transitions from widespread floodplain environments to the terra firme–dominated landscapes described below.

Paleoenvironmental reconstruction of Central Amazonia during the mid-late Pleistocene

The geological reconstruction outlined above leads to a long-term transition, at the scale of hundreds of thousands of years, from seasonally flooded environments to terra firme–dominated landscapes in Central Amazonia during the mid-late Pleistocene (Fig. 7). The process that lies behind this transition reflects successive stages of base-level fall, valley incision, and interfluve development (Fig. 9) (*29*). The regional-scale paleoenvironmental reconstruction is detailed below.

Stage I (>350 ka) was characterized by extensive low-relief alluvial plains with shallow groundwater tables (Fig. 8). Unlike the modern lowland Amazonia, where major river valleys are relatively narrow and dominated almost entirely by nutrient-rich várzea ecosystem (Fig. 1B) derived from the continual reworking of Andean sediments (with exceptions such as the Negro River), the Pleistocene paleo-alluvial plains were supplied by the same Andean-fed river systems but extended hundreds of kilometers in width. Consequently, the wide paleo-alluvial plains would have supported a broader mosaic: várzea forests flanking the main rivers, large tracts of várzea backswamps, and numerous lakes resulting from a persistently high groundwater table (Fig. 7A). In such flood-dominated settings, várzea backswamps develop away from the main channels, where surfaces remain stably waterlogged throughout the year (*35*, *75*). Areas lacking input of nutrient-rich waters would instead support nutrient-poor swamps and forests (*35*). Modern analogs include the Ucayali River south of Iquitos, where the width of the plain restricts flooding to channel-proximal areas, producing alternating belts of várzea forest and backswamps (Fig. 8). Abundant lakes would mainly be present in the center-most regions of the basin, where the trunk river flows and the topography and topographic gradients are at their lowest. Examples of lake-dominated alluvial plains may be seen in the modern reaches of the Amazon River (Solimões River downstream the Negro River mouth), the Solimões River upstream of the Japurá and upstream of the Purus, and in the Ucayali River (Fig. 8). At this stage, terra firme–dominated landscapes would be restricted to the non-depositional, topographically higher outskirts of Central Amazonia, which predate the terrace systems, such as the Subandean regions, the Guianan and Brazilian shields, and the Iranduba high (Fig. 1A) (*76*), all of which are defined geomorphologically as areas lying beyond the maximum lateral extent of Pleistocene alluvial aggradation and not affected by seasonal river-related floods.

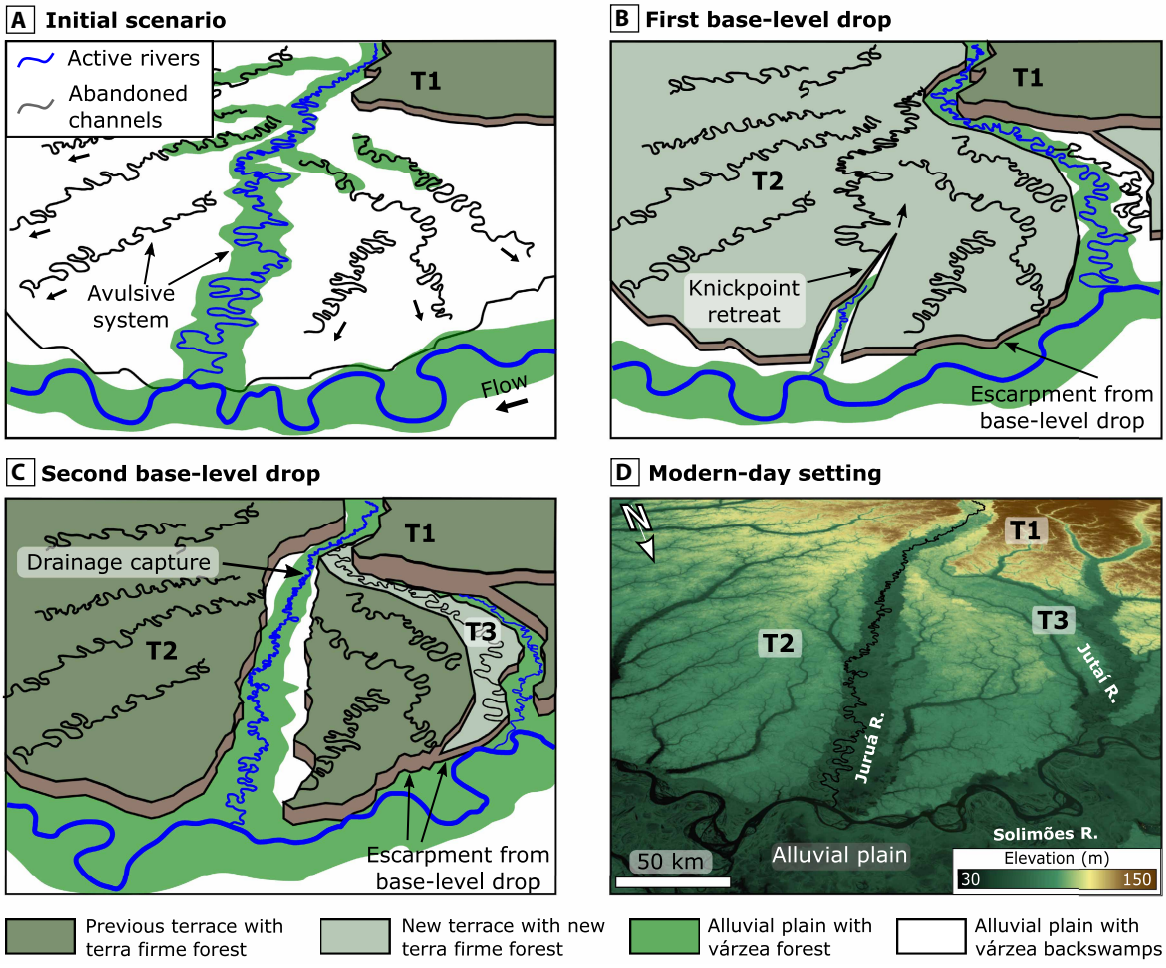

Fig. 9. Schematic evolution of the main processes associated with base-level fall events, exemplified by the perspective view of the lower Paleo-Juruá megafan from stage II to stage IV. (**A**) Fan development stage (stage II): frequent lateral shift of channel position through nodal avulsion dominates fan construction. Older terrace (T1) bears terra firme, whereas alluvial plain bears várzea forest, backswamps, and small lakes. (**B**) Onset of incision (stage III): Base-level fall triggers entrenchment of the Juruá River along its final course within the megafan, forming a new terrace (T2) colonized by terra firme forest. (**C**) Second base-level drop (stage IV): tributaries to the lower position of the Solimões River, producing valley incision and upstream retreat of knickpoints, leading to formation of a younger terrace (T3) and capture of the Juruá River into its modern course. (**D**) Digital-elevation model illustrating the current scenario of multiple terrace levels and the present alluvial plain. Note that courses of paleo-rivers and extension of várzea forest at their margins are schematic. See Fig. 1 for location (perspective view).

Stage II (350 to 90 ka) followed the first base-level fall. Valley incision lowered both flood height and groundwater table. This favored the replacement of vegetation adapted to the seasonal flooding cycle by vegetation adapted to nonflooded substrates (*35*, *75*, *77*, *78*), lastly converting former floodplain environments into interfluves now occupied by terra firme forests, which expanded from adjacent higher terrains (Fig. 7B). Each event of base-level fall leads to a net reduction of floodplain extension followed by a gradual, partial recovery due to the erosional widening of river valleys (Fig. 9). Since incision due to the erosional lowering of the main trunk river acts from the downstream end of the tributaries upward (Fig. 9), a disconnection occurs from the main várzea corridors flanking the rivers, temporarily fragmenting seasonally flooded habitats until lateral erosion reestablished wider valleys.

Stage III (90 to 45 ka) represents a further stepped-down configuration of stage II, marked by the continued expansion of terra firme environments toward the basin axis. The established incised river valleys act as barriers between the expanding terra firme areas (Fig. 7C).

Stage IV (<45 ka), the modern setting, corresponds to fully incised valleys and stabilized interfluves that host continuous terra firme forest, with várzea and igapó vegetation confined to narrow floodplains along active channels (Fig. 7D). Incision progressed until the Holocene, when aggradation within incised valleys started a new phase of floodplain deposition and expansion of seasonally flooded environments (*55*).

Thus, the transition from wide alluvial plains to incised river valleys led to the shift from seasonally flooded environments to terra firme–dominated landscapes, thereby allowing terra firme taxa to spread into the lowlands from peripheral areas such as the Fitzcarrald Arch, the Guianan and Brazilian shields, and the Andean foothills. Although there may be differences in terra firme forest composition between older high terrains and newly available terrace substrates due to variations in soil chemistry (*79*), this hypothesis explains the

existence of continuous areas of endemism whose substrates are composed of both Pleistocene deposits and older geological units (Fig. 1C). Notably, the predicted reduction of Amazonian wetlands and the respective replacement of vegetation are observed in palynological studies from core retrieved at the mouth of the Amazon River, which led to the interpretation of a reduction in Amazonian wetlands that started around 700 ka and intensified from 400 ka (*80*).

Regional and temporal context of Central Amazonia mid-late Pleistocene deposits

From a source-to-sink perspective, the lowlands of Central Amazonia form a major continental sediment repository located between the Andes and the Andean foreland system to the west and the lower Amazon valley, bounded by crystalline shields, which routes sediments to the Amazon Fan, the main marine depositional sink of the Amazon drainage basin to the east (Fig. 1A). In fluvial sequence stratigraphy, base-level rise generally promotes sediment accumulation, whereas base-level fall and lowstand conditions favor incision, erosion, and the formation of stratigraphic discontinuities (*81*–*83*). In addition to base-level controls, climatic forcing is expected to modulate fluvial stacking patterns through changes in water discharge and sediment supply, with incision typically occurring during periods of increased discharge and/or reduced sediment flux and aggradation occurring during periods of reduced discharge and/or increased sediment supply (*82*, *84*, *85*).

The Andes have acted as effective orographic barrier for Atlantic-originated moisture since at least the Miocene (*10*, *12*, *86*), and Pleistocene records from the Amazon Fan indicate that climate has exerted a control on detrital input, with Andean-derived fine-grained sediments displaying cyclic behavior correlated with climatic oscillations (*80*, *87*). These records show that climatic signals reached the Amazon Fan from the Andes, implying that water discharge variability in the Amazon drainage basin responded to regional precipitation changes (*88*) even at the orbital cycle timescale. Recent studies further show that eustatic forcing can propagate far inland in large, low-gradient river systems, with glacial-interglacial sea level oscillations influencing depositional patterns more than 1000 km from the coastline (*89*). In this way, the Central Amazonian sedimentary record may reflect depositional and erosive forcings related to climatically induced discharge variability at the scale of tens to hundreds of thousands of years (*90*) and the inland propagation of sea level oscillations at the scale of hundreds of thousands of years (*91*).

Within this regional framework, Central Amazonia records four major depositional phases (Fig. 2) separated by episodes of incision (Fig. 9), likely associated with global sea level falls (*89*). Although current geochronological constraints do not allow robust correlation of individual terrace formation stages with specific marine isotope stages (*29*), the systematic alternation between aggradation and incision across an area approaching one million square kilometers and operating at hundreds of thousands of years timescales strongly suggests modulation by mid-late Pleistocene glacial-interglacial cyclicity. The widespread synchronicity of alluvial deposition across the Amazon basin since around 15 ka, correlated with sea level rise following the Last Glacial Maximum (*55*, *92*), demonstrates that base-level changes can propagate efficiently inland despite the great distance from the coast. By analogy, earlier glacio-eustatic cycles likely exerted comparable controls on the older depositional stages identified here. This study therefore establishes a process-based framework linking erosion and aggradation in Central Amazonia to base-level fluctuations, providing the sedimentary and geomorphological framework necessary for future high-resolution chronostratigraphic analyses.

The hypothesis of tectonic control for a similar configuration has been proposed for Pleistocene fluvial systems in the Peruvian foreland that drained into the Amazonian plain and are now preserved as terrace systems supporting terra firme forest (*93*). The position of these deposits within the Andean foreland suggests that relatively recent tectonic activity was the primary local control driving these landscape changes. To some extent, the Pleistocene fluvial deposits identified in Central Amazonia may correlate with those in adjacent Peruvian Sub-Andean basins, which overlie older strata and display fining-upward fluvial successions 10 to 40 m thick (*93*). However, the precise temporal implication of this potential correlation remains uncertain, given geochronological limitations and the strong tectonic control on base-level fluctuations in the Peruvian foreland setting. In contrast, in Central Amazonia, possible tectonic deformation affecting Pleistocene deposits is mainly inferred from lineaments in remote sensing imagery and is interpreted as predominantly strike-slip in nature (*94*) and therefore unlikely to have exerted a major control on regional base-level evolution.

Implications for Central Amazonian biogeography

The paleogeographic reconstruction presented above has important implications for the availability of upland forest (terra firme) and seasonally flooded forest (várzea *and* igapó) habitats through time and for shaping the riverine barriers that now delimit the distributions of several species associated to upland terra firme forests. As a consequence, paleogeographic evolution during the mid-late Pleistocene potentially reshaped species distributions and defined current endemism patterns in lowlands of Central Amazonia (Fig. 1C).

It follows from our results that large river valleys acted as dynamic physical barriers that both restricted gene flow, acting as secondary barriers, and episodically promoted allopatric divergence among terra firme taxa in opposite interfluves through processes of valley incision and river capture. The main implications for paleobiogeographic studies are detailed below.

It follows from our results that large river valleys acted as dynamic physical barriers that restricted gene flow, functioning as secondary barriers. Episodic allopatric divergence among terra firme taxa in opposite interfluves, as well as subsequent secondary contact, may have resulted from processes of valley incision and river capture. The main implications for paleobiogeographic studies are detailed below.

Allopatric vicariance

The vicariant role of rivers originates from base-level falls that trigger knickpoint retreat and valley incision, fragmenting previously continuous terra firme forests into distinct interfluves (Fig. 9). Each episode of base-level fall generates new erosional valleys, which gradually widen and develop seasonally flooded vegetation, separating upland habitats and isolating populations of terra firme organisms on opposite margins. Such widened alluvial valleys act as a barrier for terra firme taxa (*4*, *37*, *41*). The effectiveness of base-level falls in promoting speciation would rely on the extension and duration of incision and width of the seasonally flooded environments formed within the incised valleys. Because base-level lowering is initiated at the trunk river and incision propagates upstream via knickpoint migration, this mechanism predicts a higher probability of river capture in the lower reaches of tributaries than in their more distal headwater segments (Fig. 9). Consequently, these downstream segments

may have acted as less persistent biogeographic barriers over time than the middle portions of the same rivers, contrary to what is generally assumed in tests of the riverine barrier hypotheses (*8*).

Secondary contact and mixed endemism

River valleys act as long-lived but not permanent barriers to dispersal. When base-level falls and incision propagates upstream, subsequent episodes of river capture may alter drainage patterns (Fig. 9). When a river is diverted into a different location downstream, the former valley, with its várzea corridor, is abandoned. Once the valley floor becomes colonized by terra firme vegetation, previously isolated populations may reestablish contact, generating zones of hybridization or "suture zones." The contact between the Napo and Jaú areas of endemism is a clear example of a suture zone that may be explained by this process (Fig. 7D). The localized and sequential nature of these capture events may account for the temporal mismatches observed among divergence dates of sister taxa distributed across major rivers (*19*). Thus, alternating phases of isolation and reconnection would have created a complex spatial and temporal mosaic of evolutionary processes across Amazonian landscapes, which may explain areas of mixed endemism, where old and new evolutionary lineages are found (*7*, *23*). This process may potentially affect even terra firme taxa to which crossing the river valley barrier is more difficult, given that populations may be passively transferred to the opposite margin (Fig. 9).

Riverine barrier hypothesis

Given that molecular divergence times among terra firme species are generally older than the ages of terrace formation (*4*, *6*, *17*, *29*, *32*), the role of mid-late Pleistocene river valleys was likely to spatially reorganize previous population subdivisions rather than initiate speciation, acting as a dynamic physical dispersal barrier (Fig. 10). While the vicariant role of the river may have occurred in headwaters at a time that predates the studied Pleistocene landscape changes and may explain reported discrepancies in speciation ages among areas of endemism (Fig. 9), the large rivers now separating the areas of endemism in the lowlands of Central Amazonia are here regarded as secondary barriers, or meeting points (*16*), of species from the distinct areas of endemism. In the lowlands, the landscape reconstruction (Fig. 7) shows that valleys separating terra firme regions were substantially wider than in the modern landscape, gradually narrowing through time (Fig. 10), and that terra firme within each area of endemism expanded in area toward Central Amazonia, increasing habitat availability for terra firme specialist populations. Consequently, many modern river boundaries that appear to be easily crossable still coincide with persistent ecological and genetic discontinuities (*15*, *17*, *18*, *21*, *22*, *24*). This suggests that current areas of endemism result from long-term ecological structuring within evolving landscapes during the mid-late Pleistocene, maintaining their unique endemic taxa even if present-day river barriers are weak or ephemeral (*16*, *17*, *19*–*22*). From this model, we support the conclusion that speciation of terra firme taxa must have occurred in the outskirts of Central Amazonia (*16*, *23*), at a time when the lowlands were occupied by hundreds-of-kilometers-wide alluvial plains and large rivers that frequently shifted position through nodal avulsions. These taxa subsequently dispersed toward the lowlands following base-level drops and the expansion of terra firme forests, leading to their present-day distribution in adjacent interfluves (Fig. 10).

Aquatic environments

From an aquatic and wetland perspective, the long-term persistence of large river systems implies the continued occurrence of the annual flood pulse within their floodplains. The temporal continuity of this process allowed várzea ecosystems to remain widespread along their floodplain corridors since at least the mid-late Pleistocene, providing a unique evolutionary setting for aquatic and semiaquatic biota. For floodplain trees, this environmental continuity creates stable adaptive conditions of seasonal flooding, driving the evolution (*35*) of floodplain specialists (*26*) and even endemic várzea tree species (*25*). This phenomenon is globally unique, as no other major floodplain system is known to host flood-adapted, endemic tree lineages (*25*). Moreover, the temporal continuity of várzea landscapes implies the long-term maintenance of refugia for drought-sensitive terrestrial taxa capable of tracking shallow groundwater tables (*25*, *33*) during phases of reduced precipitation in Amazonia (*90, 95*). River channels and their connected várzea environments also provide dispersal routes for fishes and floodplain-related organisms (*35*, *55*). In the case of fish communities, the reorganization of drainage networks through knickpoint retreats (Fig. 9) would lead to episodic isolation of formerly connected drainages, promoting allopatric divergence and speciation (*96*). Such processes are consistent with observed patterns of fish diversity and endemism in Amazonian rivers, where many lineages are strongly related to individual subbasin drainages and diversification appears linked to long-term geomorphological compartmentalization (*97*).

Testable hypothesis derived from the paleogeographic model

The paleogeographic interpretation of the terrace systems of Central Amazonia reveals that the role of rivers in changing the physical landscape goes far beyond the simple idea of horizontally shifting the position of barriers to gene flow through river dynamics (Fig. 7). Channel position shifts due to nodal avulsion are known to take place at the hundred-year scale in modern large-scale distributive fluvial systems (*58*, *73*, *74*), and such fast dynamics would prevent any riverine barrier effect. Instead, a more fundamental process controls long-term habitat reorganization, that is the vertical adjustment of river profiles through base-level changes leading to erosion or sediment accumulation, which drives the merged expansion or fragmentation of upland environments (Fig. 9).

In that sense, the model presented herein predicts that events of base-level fall, due to the upstream readjustment of the river profile to a lower sea level, an increase in discharge of the main trunk river, or the combined effect of both processes (*49*, *55*, *86*, *92*), result in the incision of a deeper valley on previous deposited sediments, thus causing the incision of tributaries and the lowering of the local groundwater table. The process results in the expansion of terra firme from older upland areas at the expense of aquatic environments and mosaics of seasonally flooded forest and water-logged, nutrient-poor vegetation, as has been occurring for the last few hundred thousand years (Fig. 7).

Viewed within a broad temporal framework, these incision and aggradation cycles appear broadly consistent with variations in base level and climate within a hundred thousand years span during the mid-late Pleistocene. Given that deposition in modern alluvial plains has been shown to correlate with the post–Last Glacial Maximum highstand (*55*), it is plausible that the major stages outlined in this study reflect a similar process. However, because of limited data and geochronological uncertainties, a detailed correlation of depositional stages with specific controls on base-level change, such as glacial-interglacial cycles, is not attempted here. Rather, this study provides a framework for future research on this topic.

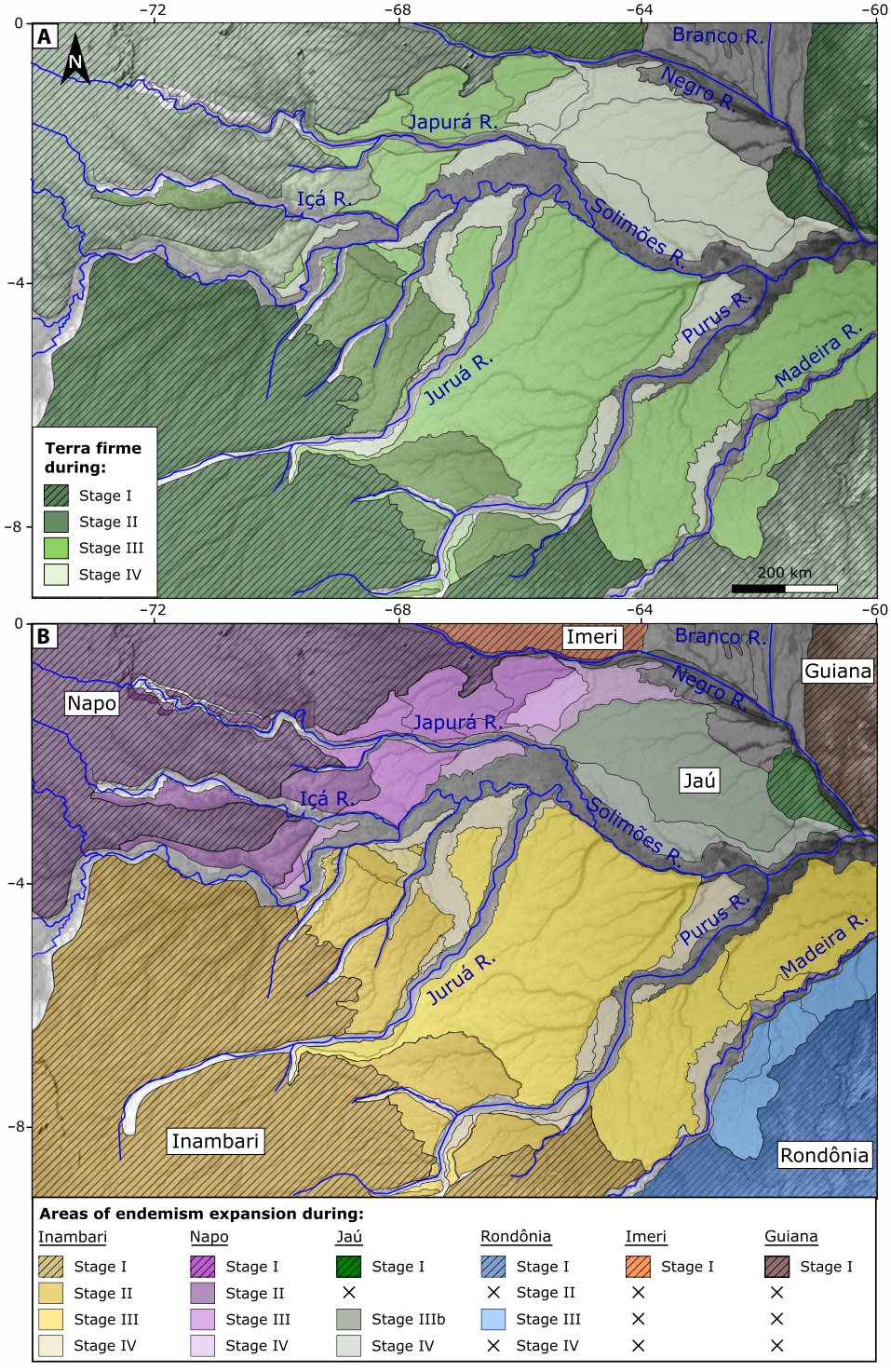

Fig. 10. Expansion of terra firme and areas of endemism during the mid-late Pleistocene. (**A**) Progressive advance of terra firme from peripheral uplands toward the central lowlands from stage I to stage IV, following successive base-level drops and terrace formation as shown in Fig. 7. (**B**) Schematic representation of the corresponding expansion of areas of endemism, showing how biogeographic boundaries shifted as a consequence of the progressive inland spread of terra firme. Shaded colors in (A) and (B) indicate the presence of terra firme and areas of endemism that predate the studied deposits.

The model presented herein stipulates that base-level drops resulted not only in the growth of terra firme but also in the expansion of areas of endemism during the mid-late Pleistocene, which followed the expansion of the terra firme from the upland areas, where the biota was already isolated in separated interfluves by the upstream reaches of the same major rivers (Fig. 10). Gene flow across channels would hardly be prevented if it was not for the role of the incised valleys that separate interfluves. Within these valleys, wide tracts of seasonally flooded environments subject to dynamic changes in the position of channels and bars act as barriers to terra firme taxa dispersion (*4*, *37*, *41*).

The main testable hypotheses derived from our model are as follows:

1) Populations of terra firme taxa expanded to lowland Central Amazonia as previously isolated units bounded by the upland reaches of the main rivers. The process of creation of new terra firme environments by river incision kept those populations isolated as they expanded on the extended interfluves.

2) These population expansion events occurred successively during events of base-level fall (either due to the inland propagation of sea level oscillations or to increased river discharge) that are recorded in the stratigraphy of mid-late Pleistocene deposits. The last events occurred as late as 45 ka (*29*).

3) During the mid-late Pleistocene, repeated episodes of relative base-level fall across the alluvial plains progressively reduced both seasonally flooded vegetation (including flooded forests and waterlogged open environments) and aquatic systems. These events promoted a stepwise expansion of terra firme from the Andean flanks and adjacent shield areas through valley incision and groundwater lowering. Each phase of incision caused an abrupt contraction of flooded and aquatic environments, followed by partial recovery during subsequent valley widening and sediment aggradation. Overall, the long-term trajectory reflects a net expansion of terra firme at the expense of both seasonally flooded and aquatic habitats.

Current limitations mainly concern chronological resolution. Additional geochronological constraints are required to refine the history of landscape evolution in Central Amazonia during the Pleistocene. Nonetheless, geological and geomorphological evidence supports a dynamic and stepwise landscape evolution throughout the mid-late Pleistocene, with important implications for paleobiogeographic studies.

MATERIALS AND METHODS

Experimental design

The objective of this study was to evaluate whether major rivers in Central Amazonia have acted as persistent biogeographic barriers throughout the mid-late Pleistocene by reconstructing the fluvial landscape evolution and assessing its implications for habitat distribution and areas of endemism. To address this, we designed an integrative geological approach combining remote sensing, quantitative geomorphological measurements, field observations, and chronological constraints.

First, we mapped terrace surfaces and paleochannel deposits using a SRTM-based DEM to identify preserved fluvial landforms and their spatial relationships. Second, we quantified planform depositional element dimensions (scroll bar radii of curvature) on both terrace surfaces and modern active floodplains. These measurements allow comparison of channel sizes through time and provide a test for the presence and scale of major rivers at the time of terrace formation while also yielding plan view paleoflow indicators.

Third, we conducted targeted field campaigns guided by the DEM-mapped features, where we described sedimentary facies and architectural elements to verify the geomorphological interpretations and to identify depositional environments represented by the terrace successions and obtain high-resolution paleoflow measurements from cross-stratifications.

Last, we compiled and evaluated available geochronological ages (OSL and radiocarbon) from published sources and our data to constrain the relative chronology of landform development and the absolute timing of terrace deposition. These datasets collectively enabled reconstruction of fluvial dynamics across the mid-late Pleistocene and assessment of the long-term persistence or reorganization of major rivers relevant to the riverine barrier hypothesis.

Terrace stratigraphy

Fluvial terraces of Central Amazonia were mapped and correlated using interpretation of satellite imagery (Landsat) and SRTM-derived DEM. The recognition of individual gently dipping surfaces of flat terrace tops, bounded by erosional escarpments truncating older surfaces. The cross-cutting relationships between these surfaces established a relative chronology of terrace formation. Depositional ages were compiled from published datasets, including OSL ages on detrital sediments and radiocarbon (^{14}C) ages on organic material.

Field-based sedimentology

Field investigations targeted representative successions of distinct terrace generations during five field campaigns conducted in the dry seasons from 2015 to 2023. Stage II and III successions were examined in exposures dated by (*27*) and in additional outcrops of the Juruá megafan along the Solimões River (between Coari and São Francisco do Içá). Equivalent terrace stages were also documented in the Japurá valley (between Japurá and Tefé) and in the Purus valley (between Boca do Acre and Lábrea). Sedimentological analysis followed the architectural element approach in (*98*), integrating vertical profiles, lithofacies descriptions, and interpretation of hydrodynamic structures to reconstruct depositional environments.

Measurement of scroll bars radii of curvature

Radii of curvature of scroll bars were measured in areas representing modern or very recent formation of bars within the active alluvial plains and were selected to be close to a gauging station with available water discharge data. For each individual scroll bar in the recent alluvial plain, five georeferenced points were collected in Google Earth based on underlying Landsat imagery and processed SRTM digital elevation data, composing a single kml file for each area. These kml files were then processed with a Python code written for that purpose (see data S2 in the Supplementary Materials), which calculated radii of curvature from sets of three points using the law of cosines, yielding three estimates per bar. Mean bar radius of curvature was determined for each site. The same procedure was applied to preserved bar structures identified on terrace surfaces. All kml files are presented in the Supplementary Materials (data S2).

Statistical analysis

The method outlined above enabled quantitative comparison of bar morphometrics between modern alluvial plains and Pleistocene terrace deposits. For each site, basic descriptive statistics were computed

to summarize variability in radii of curvature, and boxplots were used to visually assess differences in central tendency and spread.

To assess whether mean scroll bar radii differed between modern and Pleistocene samples, we used a nonparametric bootstrap test for equality of means. For each comparison, let x represent the Pleistocene terrace sample and y the corresponding modern river or tributary sample. Values equal to 0.0 were treated as missing and removed from both samples before the analysis, to avoid biasing the estimates when zeros represent absent or invalid measurements. The observed test statistic is the difference in sample means: $\Delta\_obs = \text{mean}(x) - \text{mean}(y)$. Under the null hypothesis H_0: $\mu x = \mu y$, both samples are assumed to originate from the same underlying distribution, so all observations were pooled. We then generated n_boot = 10,000 bootstrap replicates by repeatedly resampling, with replacement, from the pooled data, splitting each resample into groups of sizes n1 and n2, and recomputing the mean difference. This produced an empirical null distribution of Δ. The P value was calculated as the proportion of bootstrap replicates as or more extreme than Δ_obs, using either a two-sided or one-sided alternative as appropriate. This provides a distribution-free assessment of whether the observed mean difference could arise from sampling variability (table S1).

To assess differences in the full distributional shape, we also used the two-sample KS test, which compares the empirical cumulative distribution functions (ECDFs) of the two samples. The KS statistic D is the maximum vertical distance between the ECDFs. Unlike the bootstrap mean test, the KS test is sensitive to changes in central tendency, spread, skewness, and tail behavior. Its associated P value gives the probability, under the null hypothesis of identical continuous distributions, of observing a distance D as large or larger than the one measured. Together, the bootstrap and KS tests provide complementary assessments of differences in bar radius distributions (table S1). All used codes are included in the Supplementary Materials (data S2).

Supplementary Materials

The PDF file includes:

Figs. S1 to S5
Tables S1 and S2
Legends for data S1 and S2

Other Supplementary Material for this manuscript includes the following:

Data S1 and S2

REFERENCES

1. A. R. Wallace, On the monkeys of the Amazon. *Ann. Mag. Nat. Hist.* **14**, 451–454 (1852).
2. J. Cracraft, Historical biogeography and patterns of differentiation within the south American avifauna: Areas of endemism. *Ornithol. Monogr.* **36**, 49–84 (1985).
3. M. A. Rego, G. Del-Rio, R. T. Brumfield, Subspecies-level distribution maps for birds of the Amazon basin and adjacent areas. *J. Biogeogr.* **51**, 14–28 (2023).
4. C. C. Ribas, A. O. Sawakuchi, R. P. Almeida, F. N. Pupim, M. A. Rego, R. Batista, L. L. Knowles, The role of rivers in the origin and future of Amazonian biodiversity. *Nat. Rev. Biodivers.* **1**, 14–31 (2025).
5. J. Salo, R. Kalliola, I. Häkkinen, Y. Mäkinen, P. Niemelä, M. Puhakka, P. D. Coley, River dynamics and the diversity of Amazon lowland forest. *Nature* **322**, 254–258 (1986).
6. C. C. Ribas, A. Aleixo, A. C. R. Nogueira, C. Y. Miyaki, J. Cracraft, A paleobiogeographic model for biotic diversification within Amazonia over the past three million years. *Proc. Biol. Sci.* **279**, 681–689 (2012).
7. L. J. Musher, M. Giakoumis, J. Albert, G. Del-Rio, M. Rego, G. Thom, A. Aleixo, C. C. Ribas, R. T. Brumfield, B. T. Smith, J. Cracraft, River network rearrangements promote speciation in lowland Amazonian birds. *Sci. Adv.* **14**, eabn1099 (2022).
8. C. C. Ribas, S. C. Fritz, P. A. Baker, The challenges and potential of geogenomics for biogeography and conservation in Amazonia. *J. Biogeogr.* **49**, 1839–1847 (2022).
9. J. Figueiredo, C. Hoorn, P. van der Ven, E. Soares, Late Miocene onset of the Amazon River and the Amazon deep-sea fan: Evidence from the Foz do Amazonas Basin. *Geology* **37**, 619–622 (2009).
10. C. Hoorn, G. R. Bogotá-A, M. Romero-Baez, E. I. Lammertsma, S. G. A. Flantua, E. L. Dantas, R. Dino, D. A. do Carmo, F. Chemale Jr., The Amazon at sea: Onset and stages of the Amazon River from a marine record, with special reference to Neogene plant turnover in the drainage basin. *Glob. Planet. Change* **153**, 51–65 (2017).
11. E. E. van Soelen, J. H. Kim, R. V. Santos, E. L. Dantas, F. V. de Almeida, J. P. Pires, M. Rodaz, J. S. Sinninghe, J. S. S. Damsté, A 30 Ma history of the Amazon River inferred from terrigenous sediments and organic matter on the Ceará Rise. *Earth Planet. Sci. Lett.* **474**, 40–48 (2017).
12. C. Hoorn, F. P. Wesselingh, H. Ter Steege, M. A. Bermudez, A. Mora, J. Sevink, I. Sanmartín, A. Sanchez-Meseguer, C. L. Anderson, J. P. Figueiredo, C. Jaramillo, D. Riff, F. R. Negri, H. Hooghiemstra, J. Lundberg, T. Stadler, T. Särkinen, A. Antonelli, Amazonia through time: Andean uplift, climate change, landscape evolution, and biodiversity. *Science* **330**, 927–931 (2010).
13. E. M. Latrubesse, M. Cozzuol, S. A. F. Silva-Caminha, C. A. Rigsby, M. L. Absy, C. Jaramillo, The Late Miocene paleogeography of the Amazon Basin and the evolution of the Amazon River system. *Earth Sci. Rev.* **99**, 99–124 (2010).
14. C. Jaramillo, I. Romero, C. D'Apolito, G. Bayona, E. Duarte, S. Louwye, J. Escobar, J. Luque, J. D. Carrillo-Briceño, V. Zapata, A. Mora, S. Schouten, M. Zavada, G. Harrington, J. Ortiz, F. P. Wesselingh, Miocene flooding events of western Amazonia. *Sci. Adv.* **3**, e1601693 (2017).
15. J. M. Ayres, T. H. Clutton-Brock, River boundaries and species range size in Amazonian primates. *Am. Nat.* **140**, 531–537 (1992).
16. J. L. Patton, M. N. F. Da Silva, J. R. Malcolm, Gene genealogy and differentiation among arboreal spiny rats (Rodentia: Echimyidae) of the Amazon Basin: A test of the riverine barrier hypothesis. *Evolution* **48**, 1314–1323 (1994).
17. J. P. Boubli, C. C. Ribas, J. W. Lynch, M. E. Alfaro, M. N. F. Silva, G. M. Pinho, I. P. Farias, Spatial and temporal patterns of diversification on the Amazon: A test of the riverine hypothesis for all diurnal primates of Rio Negro and Rio Branco in Brazil. *Mol. Phylogenet. Evol.* **82**, 400–412 (2015).
18. A. G. Nazareno, C. W. Dick, L. G. Lohmann, Tangled banks: A landscape genomic evaluation of Wallace's riverine barrier hypothesis for three Amazon plant species. *Mol. Ecol.* **5**, 980–997 (2019).
19. L. N. Naka, R. T. Brumfield, The dual role of Amazonian rivers in the generation and maintenance of avian diversity. *Sci. Adv.* **4**, eaar8575 (2018).
20. R. M. Pirani, F. P. Werneck, A. T. Thomaz, M. L. Kenney, M. J. Sturaro, T. C. S. Ávila-Pires, P. L. V. Peloso, M. T. Rodrigues, L. L. Knowles, Testing main Amazonian rivers as barriers across time and space within widespread taxa. *J. Biogeogr.* **46**, 2444–2456 (2019).
21. G. Fordham, S. Shanee, M. Peck, Effect of river size on Amazonian primate community structure: A biogeographic analysis using updated taxonomic assessments. *Am. J. Primatol.* **82**, e23136 (2020).
22. I. Mourthé, R. R. Hilário, W. D. Carvalho, J. P. Boubli, Filtering effect of large rivers on primate distribution in the Brazilian Amazonia. *Front. Ecol. Evol.* **10**, 857920 (2022).
23. J. M. Guayasamin, C. C. Ribas, A. C. Carnaval, J. D. Carrillo, C. Hoorn, L. G. Lohmann, D. Riff, C. Ulloa Ulloa, J. S. Albert, Evolution of Amazonian biodiversity: A review. *Acta Amaz.* **54**, 1–34 (2024).
24. W. D. Helenbrook, J. W. Valdez, Role of rivers as geographical barriers in shaping molecular divergence of neotropical primates. *Biotropica* **57**, e70028 (2025).
25. F. Wittmann, E. Householder, M. T. F. Piedade, R. L. de Assis, J. Schöngart, P. Parolin, W. J. Junk, Habitat specifity, endemism and the neotropical distribution of Amazonian white-water floodplain trees. *Ecography* **36**, 690–707 (2013).
26. J. E. Householder, F. Wittmann, J. Schöngart, M. T. F. Piedade, W. J. Junk, E. M. Latrubesse, A. C. Quaresma, L. O. Demarchi, G. S. Lobo, D. P. P. Aguiar, R. L. Assis, A. Lopes, P. Parolin, I. L. Amaral, L. S. Coelho, F. D. A. Matos, D. A. L. Filho, R. P. Salomão, C. V. Castilho, J. E. Guevara-Andino, M. J. V. Carim, O. L. Phillips, D. C. López, W. E. Magnusson, D. Sabatier, J. D. C. Revilla, J. F. Molino, M. V. Irume, M. P. Martins, J. R. S. Guimarães, J. F. Ramos, D. J. Rodrigues, O. S. Bánki, C. A. Peres, N. C. A. Pitman, J. E. Hawes, E. J. Almeida, L. F. Barbosa, L. Cavalheiro, M. C. V. Santos, B. G. Luize, E. M. M. L. Novo, P. N. Vargas, T. S. F. Silva, E. M. Venticinque, A. G. Manzatto, N. F. C. Reis, J. Terborgh, K. R. Casula, F. R. C. Costa, E. N. H. Coronado, A. M. Mendoza, J. C. Montero, T. R. Feldpausch, G. A. Aymard C, C. Baraloto, N. C. Arboleda, J. Engel, P. Petronelli, C. E. Zartman, T. J. Killeen, L. M. Rincón, B. S. Marimon, B. H. Marimon-Junior, J. Schietti, T. R. Sousa, R. Vasquez, B. Mostacedo, D. D. Amaral, H. Castellanos, M. B. Medeiros, M. F. Simon, A. Andrade, J. L. Camargo, W. F. Laurance, S. G. W. Laurance, E. S. Farias, M. A. Lopes, J. L. L. Magalhães, H. E. M. Nascimento, H. L. Queiroz, R. Brienen, P. R. Stevenson, A. Araujo-Murakami, T. R. Baker, B. B. L. Cintra, Y. O. Feitosa, H. F. Mogollón, J. C. Noronha, F. R. Barbosa, R. S. Carpanedo, J. F. Duivenvoorden, M. R. Silman, L. V. Ferreira, C. Levis, J. R. Lozada, J. A. Comiskey, F. C. Draper, J. J. Toledo, G. Damasco, N. Dávila, R. García-Villacorta, A. Vicentini, F. C. Valverde, A. Alonso, L. Arroyo, F. Dallmeier, V. H. F. Gomes, E. M. Jimenez, D. Neill, M. C. P. Mora, F. A. Carvalho, F. C. Souza, K. J. Feeley,

R. Gribel, M. P. Pansonato, M. R. Paredes, J. Barlow, E. Berenguer, K. G. Dexter, J. Ferreira, P. V. A. Fine, M. C. Guedes, I. Huamantupa-Chuquimaco, J. C. Licona, T. Pennington, B. E. V. Zegarra, V. A. Vos, C. Cerón, E. Fonty, T. W. Henkel, P. Maas, E. Pos, M. Silveira, J. Stropp, R. Thomas, D. Daly, W. Milliken, G. P. Molina, I. C. G. Vieira, B. W. Albuquerque, W. Campelo, T. Emilio, A. Fuentes, B. Klitgaard, J. L. M. Pena, P. F. Souza, J. S. Tello, C. Vriesendorp, J. Chave, A. Di Fiore, R. R. Hilário, L. O. Pereira, J. F. Phillips, G. Rivas-Torres, T. R. van Andel, P. von Hildebrand, W. Balee, E. M. Barbosa, L. C. M. Bonates, H. P. D. Doza, R. Z. Gómez, T. Gonzales, G. P. G. Gonzales, B. Hoffman, A. B. Junqueira, Y. Malhi, I. P. A. Miranda, L. F. Mozombite-Pinto, A. Prieto, A. Rudas, A. R. Ruschel, N. Silva, C. I. A. Vela, S. Zent, E. L. Zent, A. Cano, Y. A. C. Márquez, D. F. Correa, J. B. P. Costa, B. M. Flores, D. Galbraith, M. Holmgren, M. Kalamandeen, M. T. Nascimento, A. A. Oliveira, H. Ramirez-Angulo, M. Rocha, V. V. Scudeller, R. Sierra, M. Tirado, M. N. Umaña, G. van der Heijden, E. V. Torre, M. A. A. Reategui, C. Baider, H. Balslev, S. Cárdenas, L. F. Casas, W. Farfan-Rios, C. Ferreira, R. Linares-Palomino, C. Mendoza, I. Mesones, G. A. Parada, A. Torres-Lezama, L. E. U. Giraldo, D. Villarroel, R. Zagt, M. N. Alexiades, E. A. Oliveira, K. Garcia-Cabrera, L. Hernandez, W. P. Cuenca, S. Pansini, D. Pauletto, F. R. Arevalo, A. F. Sampaio, E. H. V. Sandoval, L. V. Gamarra, H. ter Steege, One sixth of Amazonian tree diversity is dependent on river floodplains. *Nat. Ecol. Evol.* **8**, 901–911 (2024).
27. A. C. R. Nogueira, R. Silveira, J. T. F. Guimarães, Neogene–Quaternary sedimentary and paleovegetation history of the eastern Solimões Basin, central Amazon region. *J. South Am. Earth Sci.* **46**, 89–99 (2013).
28. D. F. Rossetti, M. C. L. Cohen, S. H. Tatumi, A. O. Sawakuchi, É. H. Cremon, J. C. R. Mittani, T. C. Bertani, C. J. A. S. Munita, D. R. G. Tudela, M. Yee, G. Moya, Mid–late Pleistocene OSL chronology in western Amazonia and implications for the transcontinental Amazon pathway. *Sediment. Geol.* **330**, 1–15 (2015).
29. F. N. Pupim, A. O. Sawakuchi, R. P. Almeida, C. C. Ribas, A. K. Kern, G. A. Hartmann, C. M. Chiessi, L. N. Tamura, T. D. Mineli, J. F. Savian, C. H. Grohmann, D. J. Bertassoli Jr., A. G. Stern, F. W. Cruz, J. Cracraft, Chronology of terra firme formation in Amazonian lowlands reveals a dynamic Quaternary landscape. *Quat. Sci. Rev.* **210**, 154–163 (2019).
30. S. M. Silva, A. T. Peterson, L. Carneiro, T. C. T. Burlamaqui, C. C. Ribas, T. Sousa-Neves, L. S. Miranda, A. M. Fernandes, F. M. d'Horta, L. E. Araújo-Silva, R. Batista, C. H. M. M. Bandeira, S. M. Dantas, M. Ferreira, D. M. Martins, J. Oliveira, T. C. Rocha, C. H. Sardelli, G. Thom, P. S. Rêgo, M. P. Santos, F. Sequeira, M. Vallinoto, A. Aleixo, A dynamic continental moisture gradient drove Amazonia bird diversification. *Sci. Adv.* **5**, eaat5752 (2019).
31. E. D. Schultz, C. W. Burney, R. T. Brumfield, E. M. Polo, J. Cracraft, C. C. Ribas, Systematics and biogeography of the Automolus infuscatus complex (Aves: Furnariidae): Cryptic diversity reveals western Amazonia as the origin of a transcontinental radiation. *Mol. Phylogenet. Evol.* **107**, 503–515 (2017).
32. H. Byrne, J. W. Lynch Alfaro, I. Sampaio, I. Farias, H. Schneider, T. Hrbek, J. P. Boubli, Titi monkey biogeography: Parallel Pleistocene spread by Plecturocebus and Cheracebus into a post-Pebas Western Amazon. *Zool. Scr.* **47**, 499–517 (2018).
33. P. A. Baker, S. C. Fritz, C. W. Dick, A. J. Eckert, B. K. Horton, S. Manzoni, C. C. Ribas, C. N. Garzione, D. S. Battisti, The emerging field of geogenomics: Constraining geologic problems with genetic data. *Earth Sci. Rev.* **135**, 38–47 (2014).
34. H. Sioli, *The Amazon* (Monographiae Biologicae 56, Springer, 1984). https://doi.org/10.1007/978-94-009-6542-3_5.
35. W. J. Junk, M. T. F. Piedade, J. Schöngart, M. Cohn-Haft, J. M. Adeney, F. Wittmann, A classification of major naturally occurring Amazonian lowland wetlands. *Wetlands* **31**, 623–640 (2011).
36. T. O. Laranjeiras, C. C. Ribas, M. Cohn-Haft, Patterns of endemism in Amazonian floodplain birds. *Perspect. Ecol. Conserv.* **22**, 306–314 (2024).
37. C. A. Peres, J. L. Patton, M. N. Da Silva, Riverine barriers and gene flow in Amazonian saddle-back tamarins. *Folia Primatol.* **67**, 113–124 (1996).
38. A. Aleixo, Historical diversification of a terra-firme forest bird superspecies: A phylogeographic perspective on the role of different hypotheses of Amazonian diversification. *Evolution* **58**, 1303–1317 (2004).
39. S. H. Borges, J. M. C. Da Silva, A new area of endemism for Amazonian birds in the Rio Negro basin. *Wilson J. Ornithol.* **124**, 15–23 (2012).
40. M. G. Harvey, A. Aleixo, C. C. Ribas, R. T. Brumfield, Habitat association predicts genetic diversity and population divergence in Amazonian birds. *Am. Nat.* **190**, 631–648 (2017).
41. G. Del-Rio, M. J. Mutchler, B. Costa, A. E. Hiller, G. Lima, B. Matinata, J. F. Salter, L. F. Silveira, M. A. Rego, D. C. Schmitt, Birds of the Juruá River: Extensive várzea forest as a barrier to terra firme birds. *J. Ornithol.* **162**, 565–577 (2021).
42. L. F. G. Almeida, "A drenagem festonada e seu significado fotogeológico," in *Proceedings of the XXVIII Brazilian Congress of Geology 7* (Sociedade Brasileira de Geologia, 1974), pp. 175–197.
43. E. H. Hayakawa, D. F. Rossetti, M. M. Valeriano, Applying DEM-SRTM for reconstructing a late Quaternary paleodrainage in Amazonia. *Earth Planet. Sci. Lett.* **297**, 262–270 (2010).
44. K. Ruokolainen, G. M. Moulatlet, G. Zuquim, C. Hoorn, H. Tuomisto, Geologically recent rearrangements in central Amazonian river network and their importance for the riverine barrier hypothesis. *Front. Biogeogr.* **11**, e45046 (2019).
45. C. P. Galeazzi, R. P. Almeida, A. H. Do Prado, Linking rivers to the rock record: Channel patterns and paleocurrent circular variance. *Geology* **49**, 1402–1407 (2021).
46. G. P. Williams, Paleohydrological methods and some examples from Swedish fluvial environments II. River meanders. *Geogr. Ann. Ser. A* **66**, 89–102 (1984).
47. S. M. Hubbard, D. G. Smith, H. Nielsen, D. A. Leckie, M. Fustic, R. J. Spencer, L. Bloom, Seismic geomorphology and sedimentology of a tidally influenced river deposit, Lower Cretaceous Athabasca oil sands, Alberta, Canada. *AAPG Bull.* **95**, 1123–1145 (2011).
48. A. T. Hayden, M. P. Lamb, Fluvial sinuous ridges of the Morrison Formation, USA: Meandering, scarp retreat, and implications for Mars. *J. Geophys. Res. Planets* **125**, e2020JE006470 (2020).
49. A. H. Do Prado, R. P. Almeida, C. P. Galeazzi, V. Sacek, F. Schlunegger, Climate changes and the formation of fluvial terraces in central Amazonia inferred from landscape evolution modeling. *Earth Surf. Dynam.* **10**, 457–471 (2022).
50. E. M. Latrubesse, E. Franzinelli, The Holocene alluvial plain of the middle Amazon River, Brazil. *Geomorphology* **44**, 241–257 (2002).
51. E. M. Latrubesse, E. Franzinelli, The late Quaternary evolution of the Negro River, Amazon, Brazil: Implications for island and floodplain formation in large anabranching tropical systems. *Geomorphology* **70**, 372–397 (2005).
52. E. A. A. Soares, S. H. Tatumi, C. Riccomini, OSL age determinations of Pleistocene fluvial deposits in central Amazonia. *An. Acad. Bras. Ciênc.* **82**, 691–699 (2010).
53. D. F. Rossetti, M. C. L. Cohen, T. C. Bertani, E. H. Hayakawa, J. D. S. Paz, D. F. Castro, Y. Friaes, Late Quaternary fluvial-terrace evolution in the main southern Amazonian tributary. *Catena* **116**, 19–37 (2014).
54. E. S. Gonçalves Junior, E. A. A. Soares, H. Tatumi, M. Yee, J. C. R. Mittani, Pleistocene–Holocene sedimentation of Solimões–Amazon fluvial system between the tributaries Negro and Madeira, central Amazon. *Braz. J. Geol.* **46**, 167–180 (2016).
55. A. O. Sawakuchi, E. D. Schultz, F. N. Pupim, D. J. Bertassoli Jr., D. F. Souza, D. F. Cunha, C. E. Mazoca, M. P. Ferreira, C. H. Grohmann, I. D. Wahnfried, C. M. Chiessi, F. W. Cruz, R. P. Almeida, C. C. Ribas, Rainfall and sea level drove the expansion of seasonally flooded habitats and associated bird populations across Amazonia. *Nat. Commun.* **13**, 4945 (2022).
56. C. E. E. M. Mazoca, "Reconstruction of Pleistocene alluvial systems in central Amazonia," thesis, University of São Paulo, Sao Paulo, SP (2023).
57. N. Espurt, P. Baby, S. Brusset, M. Roddaz, W. Hermoza, J. Barbarand, "The Nazca Ridge and uplift of the Fitzcarrald Arch: Implications for regional geology in northern South America," in *Amazonia: Landscape and Species Evolution*, C. Hoorn, F. Wesselingh, Eds. (Wiley-Blackwell, 2009), chap. 6. https://doi.org/10.1002/9781444306408.ch6.
58. R. Slingerland, N. D. Smith, River avulsions and their deposits. *Annu. Rev. Earth Planet. Sci.* **32**, 257–285 (2004).
59. R. P. Almeida, C. P. Galeazzi, B. T. Freitas, L. Janikian, M. Ianniruberto, A. Marconato, Large barchanoid dunes in the Amazon River and the rock record: Implications for interpreting large river systems. *Earth Planet. Sci. Lett.* **454**, 92–102 (2016).
60. C. P. Galeazzi, R. P. Almeida, C. E. M. Mazoca, J. L. Best, B. T. Freitas, M. Ianniruberto, J. Cisneros, L. N. Tamura, The significance of superimposed dunes in the Amazon River: Implications for how large rivers are identified in the rock record. *Sedimentology* **65**, 2388–2403 (2018).
61. J. Cisneros, J. Best, T. van Dijk, R. P. D. Almeida, M. Amsler, J. Boldt, B. Freitas, C. Galeazzi, R. Huizinga, M. Ianniruberto, H. Ma, A. Nittouer, K. Oberg, O. Orfeo, D. Parsons, R. Szupiany, P. Wang, Y. Zhang, Dunes in the world's big rivers are characterized by low-angle lee-side slopes and a complex shape. *Nat. Geosci.* **13**, 156–162 (2020).
62. L. N. Tamura, R. P. Almeida, C. P. Galeazzi, B. T. Freitas, M. Ianniruberto, A. H. Prado, Upper-bar deposits in large Amazon rivers: Occurrence, morphology and internal structure. *Sediment. Geol.* **387**, 1–17 (2019).
63. R. P. Almeida, C. P. Galeazzi, J. Best, M. Ianniruberto, A. H. Do Prado, L. Janikian, C. E. M. Mazoca, L. N. Tamura, A. Nicholas, Morphodynamics and depositional architecture of mid-channel bars in large Amazonian rivers. *Sedimentology* **71**, 1591–1614 (2024).
64. J. S. Bridge, *Rivers and Floodplains: Forms, Processes, and Sedimentary Record* (Blackwell Publishing, 2003).
65. T. C. Bicudo, V. Sacek, R. P. Almeida, J. M. Bates, C. C. Ribas, Andean tectonics and mantle dynamics as a pervasive influence on Amazonian ecosystems. *Sci. Rep.* **9**, 16879 (2019).
66. C. Hoorn, Fluvial palaeoenvironments in the intracratonic Amazonas Basin (Early Miocene-early Middle Miocene, Colombia). *Palaeogeogr. Palaeoclimatol. Palaeoecol.* **109**, 1–54 (1994).
67. A. P. Linhares, M. I. F. Ramos, V. C. S. Gaia, Y. S. Friaes, Integrated biozonation based on palynology and ostracods from the Neogene of Solimões Basin, Brazil. *J. South Am. Earth Sci.* **91**, 57–70 (2019).
68. R. G. Maia, H. K. Godoy, H. S. Yamaguti, P. A. Moura, F. S. Costa, M. A. Holanda, J. B. S. Costa, "Projeto de carvão no Alto Solimões" (Tech. Rep. CPRM-DNPM, 1977).
69. A. K. Kern, M. Gross, C. P. Galeazzi, F. N. Pupim, A. O. Sawakuchi, R. P. Almeida, W. E. Pillerd, G. G. Kuhlmann, M. A. S. Basei, Re-investigating Miocene age control and

paleoenvironmental reconstructions in western Amazonia (northwestern Solimões Basin, Brazil). *Palaeogeogr. Palaeoclimatol. Palaeoecol.* **545**, 109652 (2020).
70. M. J. Wilkinson, L. G. Marshall, J. G. Lundberg, M. H. Kreslavsky, "Megafan environments in Northern South America and their impact on Amazon Neogene aquatic ecosystems," in *Amazonia: Landscape and Species Evolution*, C. Hoorn, F. Wesselingh, Eds. (Wiley-Blackwell, 2009), chap. 10. https://doi.org/10.1002/9781444306408.ch10.
71. N. Filizola, J. L. Guyot, Suspended sediment yields in the Amazon basin: An assessment using the Brazilian national data set. *Hydrol. Process.* **23**, 3207–3215 (2009).
72. A. J. Hartley, G. S. Weissmann, G. J. Nichols, G. L. Warwick, Large distributive fluvial systems: Characteristics, distribution, and controls on development. *J. Sediment. Res.* **80**, 167–183 (2010).
73. M. L. Assine, River avulsions on the Taquari megafan, Pantanal wetland, Brazil. *Geomorphology* **70**, 357–371 (2005).
74. R. Sinha, The great avulsion of Kosi on 18 August 2008. *Curr. Sci.* **97**, 429–433 (2009).
75. J. Ferreira-Ferreira, T. S. F. Silva, A. S. Streher, A. G. Affonso, L. F. A. Furtado, B. R. Forsberg, J. Valsecchi, H. L. Queiroz, E. M. L. de Moraes Novo, Combining ALOS/PALSAR-derived vegetation structure and inundation patterns to characterize major vegetation types in the Mamirauá Sustainable Development Reserve, central Amazon floodplain, Brazil. *Wetl. Ecol. Manag.* **23**, 41–59 (2015).
76. C. Gautheron, A. O. Sawakuchi, M. F. S. Albuquerque, C. Cabriolu, M. Parra, C. C. Ribas, F. N. Pupim, S. Schwartz, A. K. Kern, S. Gomez, R. P. Almeida, A. M. C. Horbe, F. Haurine, S. Miska, J. Nouet, N. Findling, S. B. Riffel, R. Pinna-Jamme, Cenozoic weathering of fluvial terraces and emergence of biogeographic boundaries in Central Amazonia. *Glob. Planet. Change* **212**, 103815 (2022).
77. F. Wittmann, J. Schöngart, J. C. Montero, T. Motzer, W. J. Junk, M. T. F. Piedade, H. L. Queiroz, M. Worbes, Tree species composition and diversity gradients in white-water forests across the Amazon basin. *J. Biogeogr.* **33**, 1334–1347 (2006).
78. J. Schöngart, F. Wittmann, A. F. Resende, C. Assahira, G. D. S. Lobo, J. R. D. Neves, M. Rocha, G. B. Mori, A. C. Quaresma, L. O. Demarchi, B. W. Albuquerque, Y. O. Feitosa, G. D. S. Costa, G. V. Feitoza, F. M. Durgante, A. Lopes, S. E. Trumbore, T. S. Silva, H. Ter Steege, A. L. Val, W. J. Junk, M. T. F. Piedade, The shadow of the Balbina dam: A synthesis of over 35 years of downstream impacts on floodplain forests in central Amazonia. *Aquat. Conserv. Mar. Freshw. Ecosyst.* **31**, 1117–1135 (2021).
79. M. A. Higgins, K. Ruokolainen, H. Tuomisto, N. Llerena, G. Cardenas, O. L. Phillips, R. Vasquez, M. Rasanen, Geological control of floristic composition in Amazonian forests. *J. Biogeogr.* **38**, 2136–2149 (2011).
80. A. K. Kern, T. K. Akabane, J. Q. Ferreira, C. M. Chiessi, D. A. Willard, F. Ferreira, A. O. Sanders, C. G. Silva, C. Rigsby, F. W. Cruz, G. S. Dwyer, S. C. Fritz, P. A. Baker, A 1.8 million year history of Amazon vegetation. *Quat. Sci. Rev.* **299**, 107867 (2023).
81. V. P. Wright, S. B. Marriott, The sequence stratigraphy of fluvial depositional systems: The role of floodplain sediment storage. *Sediment. Geol.* **86**, 203–210 (1993).
82. K. W. Shanley, P. J. McCabe, Perspectives on the sequence stratigraphy of continental strata. *AAPG Bull.* **78**, 544–568 (1994).
83. O. Catuneanu, H. N. Elango, Tectonic control on fluvial styles: The Balfour Formation of the Karoo Basin, South Africa. *Sediment. Geol.* **140**, 291–313 (2001).
84. J. Nie, G. Ruetenik, K. Gallagher, G. Hoke, C. N. Garzione, W. Wang, D. Stockli, H. Xiaofei, Z. Wang, Y. Wang, T. Stevens, M. Danišík, S. Liu, Rapid incision of the Mekong River in the middle Miocene linked to monsoonal precipitation. *Nat. Geosci.* **11**, 944–948 (2018).
85. S. L. Goldberg, M. J. Schmidt, J. T. Perron, Fast response of Amazon rivers to Quaternary climate cycles. *Case Rep. Med.* **126**, e2021JF006416 (2021).
86. V. Sacek, S. G. Mutz, T. C. Bicudo, R. P. Almeida, T. A. Ehlers, The Amazon paleoenvironment resulted from geodynamic, climate, and sea-level interactions. *Earth Planet. Sci. Lett.* **605**, 118033 (2023).
87. A. Govin, C. M. Chiessi, M. Zabel, A. O. Sawakuchi, D. Heslop, T. Hörner, Y. Zhang, S. Mulitza, Terrigenous input off northern South America driven by changes in Amazonian climate and the North Brazil Current retroflection during the last 250 ka. *Clim. Past* **10**, 843–862 (2014).
88. J. C. Espinoza Villar, J. Ronchail, J. L. Guyot, G. Cochonneau, F. Naziano, W. Lavado, E. Oliveira, R. Pombosa, P. Vauchel, Spatio-temporal rainfall variability in the Amazon basin countries (Brazil, Peru, Bolivia, Colombia, and Ecuador). *Int. J. Clim.* **29**, 1574–1594 (2009).
89. Z. Lai, Y. Liu, Z. Wu, Y. Xu, Z. Fang, D. R. Montgomery, Headward incision of large rivers in response to glacial sea level fall. *Sci. Adv.* **11**, eadr5446 (2025).
90. H. Cheng, A. Sinha, F. W. Cruz, X. Wang, R. L. Edwards, F. M. d'Horta, C. C. Ribas, M. Vuille, L. D. Stott, A. S. Auler, Climate change patterns in Amazonia and biodiversity. *Nat. Commun.* **4**, 1411 (2013).
91. R. M. Spratt, L. E. Lisiecki, A Late Pleistocene sea level stack. *Clim. Past* **12**, 1079–1092 (2016).
92. G. Irion, J. Müller, J. O. Morais, G. Keim, J. N. de Mello, W. J. Junk, The impact of Quaternary sea-level changes on the evolution of the Amazonian lowland. *Hydrol. Process.* **23**, 3168–3172 (2009).
93. M. Rasanen, R. Neller, J. Salo, H. Jungner, Recent and ancient fluvial deposition systems in the Amazonian foreland basin, Peru. *Geol. Mag.* **129**, 293–306 (1992).
94. D. Rossetti, The role of tectonics in the late Quaternary evolution of Brazil's Amazonian landscape. *Earth Sci. Rev.* **139**, 362–389 (2014).
95. F. Wittmann, J. E. Householder, M. T. F. Piedade, J. Schöngart, L. O. Demarchi, A. C. Quaresma, W. J. Junk, A review of the ecological and biogeographic differences of Amazonian floodplain forests. *Water* **14**, 3360 (2022).
96. M. F. Stokes, J. T. Perron, Modeling the evolution of aquatic organisms in dynamic river basins. *Case Rep. Med.* **125**, e2020JF005652 (2020).
97. T. Oberdorff, M. S. Dias, C. Jézéquel, J. S. Albert, C. C. Arantes, R. Bigorne, F. M. Carvajal-Valleros, A. De Wever, R. G. Frederico, M. Hidalgo, B. Hugueny, F. Leprieur, M. Maldonado, J. Maldonado-Ocampo, K. Martens, H. Ortega, J. Sarmiento, P. A. Tedesco, G. Torrente-Vilara, K. O. Winemiller, J. Zuanon, Unexpected fish diversity gradients in the Amazon basin. *Sci. Adv.* **5**, eaav8681 (2019).
98. A. Miall, *The Geology of Fluvial Deposits: Sedimentary Facies, Basin Analysis, and Petroleum Geology* (Springer, 1996).

Acknowledgments: We thank B. T. Freitas for the preparation of the DEM. We are grateful to L. N. Tamura and C. Breda for support during fieldwork and to A. H. Do Prado for reviewing the algorithms used in this work. We thank the editor and reviewers for constructive comments that significantly helped improve this manuscript. **Funding:** This work was supported by the Fundação de Amparo à Pesquisa do Estado de São Paulo grant 2018/23899-2 (A.O.S., C.C.R., C.E.E.M., C.P.G., F.N.P., L.J., and R.P.A.), Fundação de Amparo à Pesquisa do Estado de São Paulo grant 2022/03007-5 (F.N.P.), National Research Foundation of Korea grant RS-2022-NR070842 (C.P.G.), National Research Foundation of Korea grant RS-2023-00301976 (C.P.G.), Conselho Nacional de Desenvolvimento Científico e Tecnológico grant 430202/2018-0 (F.N.P.), Conselho Nacional de Desenvolvimento Científico e Tecnológico grant 403708/2024-9 (C.C.R.), Conselho Nacional de Desenvolvimento Científico e Tecnológico grant 305218/2009-3 (R.P.A.), Conselho Nacional de Desenvolvimento Científico e Tecnológico grant 306513/2016-1 (L.J.), Conselho Nacional de Desenvolvimento Científico e Tecnológico grant 307179/2021-4 (A.O.S.), Fundação de Amparo à Pesquisa do Estado do Amazonas grant 314860/2023-1 (C.C.R.), and National Geographic Society grant EC-52511R-18 (F.N.P.). **Author contributions:** Conceptualization: R.P.A., C.P.G., A.O.S., C.C.R., F.N.P., and F.W. Methodology: R.P.A. and A.O.S. Investigation: R.P.A., C.P.G., L.J., F.N.P., C.E.E.M., A.O.S., C.C.R., F.T.F., and F.W. Visualization: C.P.G., R.P.A., F.T.F., and F.W. Writing—original draft: R.P.A. and C.P.G. Writing—review and editing: C.P.G., R.P.A., C.E.E.M., A.O.S., L.J., C.C.R., F.W., F.T.F., and F.N.P. Funding: R.P.A., A.O.S., and F.N.P. **Competing interests:** The authors declare that they have no competing interests. **Data, code, and materials availability:** All data and code needed to evaluate and reproduce the results in the paper are present in the paper and/or the Supplementary Materials. Geospatial datasets used in this study, including terrace mapping units and scroll bar metrics, are provided as KMZ/KML files in the Supplementary Materials (data S1 and S2). The code used to perform scroll bar measurements and associated analyses is available in the Supplementary Materials. This study did not generate new materials.

Submitted 6 December 2025
Accepted 10 April 2026
Published 13 May 2026
10.1126/sciadv.aee2085

ScienceAdvances

Mid-late Pleistocene evolution of fluvial landscapes in Central Amazonia: Shaping ecosystems and areas of endemism

Cristiano P. Galeazzi, Renato P. Almeida, Carlos E. E. Mazoca, Liliane Janikian, André O. Sawakuchi, Felipe T. Figueiredo, Camila C. Ribas, Florian Wittmann, and Fabiano N. Pupim

Sci. Adv. **12** (20), eaee2085. DOI: 10.1126/sciadv.aee2085